STRUCTURE OF THE ST. FRANCOIS MOUNTAINS AND SURROUNDING LEAD BELT, S.E. MISSOURI: INFERENCES FROM THERMAL IR AND OTHER DATA SETS

November, 1982

Revised: April, 1983

Final Report: HCMM Data Analysis Program

NAS5-26533

Submitted by: Raymond E. Arvidson, P.I.

Edward A. Guinness

Duane L. Bindschadler

McDonnell Center for the Space Sciences

Washington University

St. Louis, Missouri 63130

Prepared for: Goddard Space Flight Center

Greenbelt, Maryland 20771

TABLE OF CONTENTS

1. SUMMARY

Several digital data sets were registered to a common base map for southern Missouri. These registered data sets were examined in an attempt to improve our understanding of the crustal structure and the relationships between structure and Pb-Zn-Cu, Fe, Mn, and Ba ores in the area. Data included land station reading of gravity, geologic data, and Heat Capacity Mapping Mission (HCMM) images. HCMM day infrared (IR) images of Missouri displayed linear features, which parallel a newly discovered NW-SE trending Bouguer gravity low. The low may be the present expression of a failed arm of a triple junction that formed at approximately the same time as the granite-rhyolite terrain of southern Missouri. Some linear features seen on the HCMM images correspond to mapped normal faults or to drape folds over basement relief, some correspond to extensions of mapped structures, and some do not correspond to any mapped structures. The structural pattern over the gravity low suggests vertical uplift of the low density crust via isostatic readjustment and consequent fracturing of the Paleozoic sedimentary cover. The presence of a gravity low is interesting because rifts are often sites of extensive mineralization. Thus, deposits associated with the postulated Precambrian rift may have been the source rocks for the stratabound ores presently found in the Paleozoic sedimentary rocks overlying the gravity low.

HCMM thermal data were also examined in conjunction with digital topography, land use, and Landsat MSS data to understand the phenomena that produce linears on the HCMM day IR images. These analyses were

focused on the Rolla quadrangle, extending from 90^{0} to 92^{0} W. longitude and 37^{0} to 38^{0} N. latitude. National Weather Service records and the locations of major springs were also examined. Abnormally cool regions corresponding to the locations of major springs were absent in the HCMM data. Rather, daytime temperature variations were dominated by the type of vegetation, which is governed by land use. Cool areas corresponded to forests composed of oak and hickory trees and warm areas to rangeland and farmland. Evaporation of moisture from leaves probably kept the forests cool. No differential solar heating due to topography was discernable in the HCMM day IR data, even though the St. Francois Mountains (outcrops of Precambrian granites and rhyolites) have slopes as high as 20 degrees. Night IR images showed the St. Francois Mountains as the hottest regions. Interfluvial ridges, which are covered with a relatively thick (about 20m) clay and chert rich residuum, were almost as warm as the St. Francois Mountains. For the St. Francois Mountains, warm temperatures during the night may be the consequence of bedrock exposures with thermal inertias that are higher than those found in surrounding regions. The uniqueness of this interpretation, however, is compromised by the lack of concurrent meteorology data on water vapor and air temperature differences between hills and valleys.

The linear features seen in the HCMM day IR images corresponded to the narrow, flat river valleys characteristic of the region. These areas, used as cropland and as rangeland, tend to be warmer during the day than the surrounding forested slopes. The alignment of valleys with the gravity low and with mapped fractures and drape folds implies

extensive structural control of the drainage network in southern Missouri. Finally, the lack of meteorological data for the region and the modulation of the daytime temperatures by the vegetation severely compromise extraction of thermophysical values from the diurnal temperature variations. Apparent thermal inertia images, because of the daytime temperature modulation by vegetation, do not provide direct a indication of variations in geological materials.

2. INTRODUCTION

We have been pursuing relationships between the pattern, age, and origin of structural features within the Precambrian basement rocks of southern Missouri and the locations and genesis of ore deposits. The area, especially within the Rolla quadrangle (Figure 1), is a well known lead mining district, where Mississippi Valley type Pb-Zn-Cu ores have accumulated in Cambrian carbonate rocks. The ores are associated with the stromatolitic reef and back-reef facies of the carbonate rocks. The location of these facies was controlled by the location of the shoreline, which in turn was apparently controlled by the structural pattern of Precambrian outcrops. In addition, iron ores of magmatic origin can be found in the Precambrian basement rocks along fracture zones. Manganese and barium ores also are found in the region.

Structural studies of basement rocks in southern Missouri have been pursued for a considerable amount of time, and a significant amount of information has been gained on the distribution of Precambrian rock types and their ages. Few studies, however, have addressed how the structure of the region is related to the overall structural configuration of the midcontinent. In Guinness et al. (1982) (see: Appendix I) we report the discovery of a major gravity anomaly that cuts across Missouri in a NW-SE direction (Figures 2, 3, and 4). The feature is a negative free air and Bouguer anomaly, with a Bouguer anomaly amplitude of about 34 mgals. The feature is 120 to 160 km wide and extends about 700 km in length. The gravity feature may be the present expression of a Precambrian rift. HCMM day IR images were found to

exhibit linear features aligned with this structure. In this report we first review the evidence for linear features seen in HCMM day IR images. Next, we concentrate on understanding, at least on a semi-quantitative basis, the physical setting that generates the linear features on the HCMM day IR images, along with the kinds of information that can be extracted from day-night IR pairs covering southern Missouri.

3. OVERVIEW OF DATA SETS COVERING SOUTHERN MISSOURI

Our method of studying the structure of southern Missouri was to interpret HCMM day IR, night IR, and apparent thermal inertia images in the light of other data sets, primarily topography, land use, meteorological records, and Landsat MSS data. Table 1 reviews the characteristics of the HCMM sensors. HCMM images covering southern Missouri during the spring, the summer, and the early fall of 1978 (time of the HCMM mission) that are not totally obscured by clouds are listed in Table 2, together with some data on water vapor content and air temperature from National Weather Service records. Of the 12 images in Table 2, only three day IR and four night IR images showed any contrast over the Rolla quadrangle. Only two day-night pairs (6/9 - 6/10; 9/29) could be found where the surface was not obscured by atmospheric phenomena.

Data sets that were used in conjunction with HCMM images are listed in Table 3. The locations of the major springs in Missouri are shown in Figure 5. The spring locations seem to correlate with the Missouri gravity low, perhaps because ground water flow is controlled by fractures aligned with the low. Digital topography for the Rolla quadrangle was obtained from the National Cartographic Information Center (NCIC), USGS. A digitized land use map for the Rolla quadrangle was also acquired from the USGS. These two data sets were placed in image format as shown in Figures 6, 7, and 8. Figure 6 is a gray-scale image of topography for the Rolla quadrangle; Figure 7 contains the same data as a shaded relief map with the sun at 20 degrees above the

southern horizon. The highlands in the eastern half of the quadrangle are the St. Francois Mountains. These hills are outcrops of 1.3 to 1.4 billion year old granites and rhyolites (see: Appendix 1), and they form the core of an uplift known as the Ozark Plateau. The whole plateau has been dissected extensively by streams, leaving behind many interfluvial ridges. Many stream channels in the Ozark Plateau parallel the strike of the Missouri gravity low. Figure 8 is a color-coded image showing major land use patterns for the Rolla quadrangle. Two primary units are shown on the land use map. The first consists of the mixed oak-hickory hardword forests typical of the Ozarks. The forests are formed largely in the topographically rough regions. Occurring in the flatter areas, the second unit consists of open rangeland and farmland. Mine operations, such as tailing piles, also compose a non-trivial fraction of the quadrangle.

A full-resolution Landsat mosaic was constructed digitally for the Rolla quadrangle from scenes (11278-15414 and 823731-5572500) acquired in late January, 1976. Ground control points were identified on both the images and the 1 by 2 degree quadrangle topographic map. These data points were then used to transform the Landsat image to a Mercator projection. A principal component coordinate rotation was conducted on the data from the MSS bands in order to display in one image as much of the original variance as possible. The first component image retained 89% of the variance in the data. Since the four Landsat bands are highly correlated, the first component image is the average of the four original bands. The first component image is shown in Figure 9 with each picture element reduced in size by a factor of five. The

correspondence between the Landsat mosaic and the land use map is significant. The oak-hickory forests are darker than agricultural land. Clearly, land use dominates the radiance patterns seen in the Landsat data.

Useful HCMM day and night IR images are shown in Figures 10 and 11. For these figures, the images are in the original map projection (Hotine oblique Mercator) received from the Goddard Space Flight Center (GSFC). Each image has been linearly contrast enhanced. They are shown at full resolution and centered roughly over the St. Francois Mountains. The day IR images closely resemble the Landsat mosaic, which in turn closely follows the land use map shown in Figure 8. Forested areas are the coolest areas in the HCMM day IR images. On the other hand, the night IR images provide a different type of information. In the night IR images, the warmest areas are water bodies, followed by the St. Francois Mountains and the interfluvial ridges, in that order. The day and night IR scenes do not show any correlation between the locations of springs and the presence of linear, cool zones that might be expected from fracture controlled upwelling of ground water.

4. IDENTICATION OF LINEAR FEATURES IN HCMM DAY IR IMAGES

The June 9 and 10 albedo, day IR, and night IR images (Table 2) were used to identify linear features possibly related to the underlying crustal structure of the Ozark Plateau. These images were chosen because they formed a set that could be examined individually or combined into an apparent thermal inertia image. The approach we took was to map the linear features from HCMM thermal images, then to compare those features to the distribution of known faults and folds, and finally to relate the trends in the structural data to the Missouri gravity low.

The HCMM images were contrast enhanced and transformed to a Mercator projection. As discussed, the temperature patterns in the day IR scene are controlled largely by land use. The land use patterns, however, are related to topography because agricultural activity is confined to flat areas and forested land is confined largely to rugged areas. Thus, the HCMM day IR data provide some information on topography and structural features. An apparent thermal inertia (ATI) image also was constructed using the formulation of Barnes and Price (1980):

$$ATI = N(1-A)/(DAY-NIGHT)$$

where: N is a scaling constant, A is the surface albedo, and DAY-NIGHT is the temperature difference as measured in the day and night IR images. The apparent thermal inertia image, however, did not provide a significant amount of additional information, probably because the night IR and albedo data comprise only 25% and 13% of the variance contained

in the three-dimensional albedo, day IR, and night IR data set.

Figure 12 is a sketch map showing linear features identified in the HCMM day IR image. The linear features were compared to topographic maps and to Landsat MSS images in order to remove any features that were man made. Also shown in Figure 12 are folds from the Missouri structural map (McCracken, 1971) and faults from the latest geologic map of the state (Anderson, 1979). The folds are thought to be drape folds over relief produced by faults in the Precambrian basement. Most faults in the Paleozoic rocks are high-angle normal faults, although some evidence for shear movement can be found (McCracken, 1971). The linear features seen in the day IR data fall into three classes. Some linear features correspond to mapped folds and faults, some correspond to extensions of mapped structures, and some do not correspond to any mapped structure. When the linear features seen in the HCMM data are compared to topographic data, it is clear that the linear features correspond to straight, narrow stream valleys characteristic of the region. The stream valleys, typically with flat bottoms, are used for cropland and rangeland. These stream valleys tend to be warmer during the day than the surrounding forested slopes.

The location of the Missouri gravity low also is drawn on Figure 12. Most faults, folds, and linear features (as mapped from HCMM data) in the vicinity of the gravity low tend to parallel the low. Although, further away from the gravity low the azimuths of such features tend to disperse. Apparently, the basement inhomogeneity associated with the Missouri gravity low has had a pronounced influence on the pattern of structures that have propagated through the Paleozoic sedimentary cover.

The fact that the gravity feature is a low, together with the sense of movement along the faults, suggests that vertical uplift due to isostatic readjustment has occurred.

5. INTERPRETATION OF HCMM JUNE AND SEPTEMBER DAY-NIGHT PAIRS

HCMM day IR, albedo, and night IR images for June 9 and 10 and day and night IR images for September 29 were registered to a Mercator projection using 12 ground control points. Unfortunately, the albedo image for the September scene had severe periodic noise patterns that prohibited its use. Figures 13 and 14 show the contrast enhanced day and night IR images for the Rolla quadrangle. Figure 15 is a color-coded version of HCMM day with day IR values mapped to hue, night IR values mapped to saturation, and albedo mapped to intensity. The color mapping is shown schematically in Figure 16. Figure 17 illustrates an attempt to examine variations in thermal inertia using the formulation given in Barnes and Price (1980). For the September scene, the June albedo data were used.

To interpret the patterns evident in Figures 13 and 14 and to judge the utility of apparent thermal inertia variations for this region, we need to consider the physical processes and parameters producing the radiant temperature variations. The radiant temperature of the Earth's surface (in the absence of vegetation) at any given time during the diurnal cycle depends on the thermophysical properties of the materials within about one meter of the surface. The temperature also depends on the history of solar heating during the diurnal cycle, including the effects of differential solar heating from variations in slope magnitude and direction. The temperature at any given time also depends on the sensible and latent heat transfer histories. Both effects are probably of importance in a humid region such as the Ozarks. Finally, the

radiance detected by a sensor such as HCMM is a combination of surface emission filtered through the atmosphere and emission terms from the atmosphere. For the June and September day-night pairs, little meteorological data exist that are pertinent to a quantitative understanding of the history of sensible and latent heat transfer or the local atmospheric characteristics at the times of observation. The closest National Weather Service data were collected at Columbia, Missouri, located about 100 km to the west of the Rolla quadrangle. These data (Figures 18 and 19) indicate that both day and night IR images were acquired under relatively clear conditions and after a period of about one week free of precipitation.

Comparison of the day IR images and the land use map demonstrates that land use patterns are the most important control over radiant temperature variations during the afternoon. Besides open water bodies, the coolest regions correspond to the oak-hickory forests. The warmest areas correspond to rangeland and farmland, to urban areas, and to regions with mine tailing piles. No differential solar heating from slopes can be discerned, even for the hills comprising the St. Francois Mountains that have slopes ranging from 15 to 20 degrees. Apparently, latent heat transfer by evaporation from leaves in the forests keeps the forested Ozarks cool during the day.

The June night IR image shows little contrast variation, although the St. Francois Mountains and interfluvial ridges seem to be slightly warmer. On the other hand, the other useful night images, including the September scene, show the St. Francois Mountains and interfluvial ridges to be considerably warmer than the flat regions and valley sides. For

the September scene the mountains and ridges are about 5°K higher in equivalent blackbody temperature than the valleys. The hills comprising the St. Francois Mountains have a considerable extent of exposed boulders and outcrops. The soil is also typically thinner, and the forest canopy is less well developed than in surrounding regions. Examination of the digital topography and the September night IR image shows that the warm areas on the hills are not dependent on slope direction, i.e., south facing slopes are not warmer than north facing slopes. Thus, the hills may be warm because they are covered by a material with a higher thermal inertia than material found on surrounding rangeland and farmland. Interfluvial ridges in the Ozarks are typically covered with 10 to 30 meters of a clay and chert rich residuum. At the same time, the valleys have exposures of sedimentary rock and recent alluvium. Thus, there is no obvious explanation in terms of variations in the thermophysical properties of surface material that would explain the cooler valley temperatures. It is possible that the confined nature of the valleys traps cool air to produce a thermal contrast between ridges and valleys. The small amount of contrast seen in the June scene could be caused by several phenomena. Perhaps turbulent mixing of the lower atmosphere prohibited such a segregation for the June scene. Alternatively, emission from the atmosphere may have obscured the scene contrast. Lack of local meteorological data for the area compromises the uniqueness of these interpretations. It is clear, however, that apparent thermal inertia images do no provide information on thermal inertia variations for geological materials because of the complicating influence of temperature modulation by

vegetation and the possible topographic control on meteorological conditions.

Mine tailings are one type of exposed material that are free of vegetation. The mine tailing piles shown in the land use map (Figure 8) consist of large tracts of clay and silt-sized carbonate and silicate waste from lead mills. The locations of a number of the larger tailing piles are shown on full resolution Landsat images in Figure 20 and the September day IR HCMM image. Because of the fine-grained nature of the tailings, one could hypothesize that they should have a relatively low thermal inertia. They would therefore be hotter during the afternoon and cooler during the evening as compared to surrounding materials. Examination of Figure 20, however, shows that the brightest regions in the day IR image do not correlate with the location of tailing piles. Apparently, a combination of residential areas and tailing piles provide the warmer signatures. In the night IR images the tailings are indistinguishable from surrounding areas. We do not understand the night tailings signature, although the presence of small tracts of ponded water, tracts smaller than a HCMM pixel size, probably are included with the tailing piles. The water tracts and the tailings together may produce the trend of relatively warm temperature in the afternoon and temperatures similar to surrounding areas in the early morning.

6. IMPLICATIONS FOR FUTUTRE THERMAL IR REMOTE SENSING OF MIDCONTINENT

Our attempts at processing and examining HCMM IR data to extract information on variations in thermophysical properties of surface materials have been frustrating indeed. For southern Missouri, day IR brightness variations are controlled by land use patterns, with temperature modulation by the oak-hickory forests obscuring differential solar heating of slopes. During the early morning, some brightness patterns indicative of thermal inertia variation seem to occur. The St. Francois Mountains are among the warmest regions in the early morning scenes. Interfluvial ridges, which are covered by 10 to 30 meters of clay and chert rich residuum are also relatively warm. Variations in surface materials appear to be insufficient to cause ridges to be warmer than valleys. Most likely, local meteorological effects predominate, with cool air channeled into the narrow valleys of the Ozark Plateau. These land use and meteorological perturbations are difficult to remove because of both a lack of theoretical understanding of how to model the vegetation effects and a lack of meteorological observations. Future studies directed toward extracting thermophyscial properties in this region would not be of much utility until these two problems are alleviated.

7. REFERENCES CITED

Anderson, K. H., 1979, Geologic Map of Missouri, Mo. Geol. Surv., Rolla, Missouri.

Arvidson, R. E., et al., 1982, Image processing applied to gravity and topography data covering the continental U.S., EOS, V. 63, P. 216-265.

Barnes, W. L. and J. C. Price, 1980, Calibration of a satellite infrared radiometer, Applied Optics, V. 19, P. 2153-2162.

Guinness, E. A., et al., 1982, Identification of a Precambian rift through Missouri by digital image processing of geophysical and geological data, J. Geophys. Res., V. 87, P. 8529-8545.

McCracken, M. H., 1971, Structural features of Missouri, Rep. Invest. Mo. Geol. Surv., no. 44, 68 pp.

FIGURE CAPTIONS

Figure 1. Shaded relief map depicting the topography of a portion of the midcontinent with the sun placed at 20 degrees above the southern horizon. Major features include the Ouachita Mountains, the Boston Mountains, and the Mississippi Embayment (see Figure 4). The Rolla quadrangle covering a portion of the Ozark Plateau of southern Missouri is also drawn. A refers to Columbia, B to St. Louis, and C to Springfield, Missouri. Image derived from NOAA 120 samples/degree digital elevation data.

Figure 2. Filtered (i.e., interpolated) image of Bouguer anomalies for the area shown in Figure 1. Data are from the Defense Mapping Aerospace Agency and include about 100,000 samples. Processing is discussed in Arvidson et al. (1982) and in Guinness et al. (1982) (see: Appendix I). The Missouri gravity low, defined for the first time as part of our analyses, cuts NW-SE across Missouri.

Figure 3. Shaded relief map depicting Bouguer anomalies as hills and valleys. MGL stands for Missouri gravity low, while MVG is the Mississippi Valley graben. The characteristics of these two gravity anomalies are enhanced in this figure.

Figure 4. Sketch map showing the major physiographic and gravitational

anomaly signatures evident in Figures 1, 2, and 3. The intersection of the MGL and MVG is the site of two plutons, in addition to being the site of active seismicity (see: Arvidson et al., 1982; Guinness et al., 1982). Both linear structures are probably failed rifts.

Figure 5. Locations of major springs in southern Missouri, along with estimates of discharge rates. The boundaries of the MGL and the Rolla quadrangle are also shown. The pattern of springs suggests control by the underlying crustal structure. Data are from 7 1/2 minute quadrangle maps.

Figure 6. Digital topography for the Rolla quadrangle, scaled so that bright areas correspond to high elevations. The St. Francois Mountains are outcrops of Precambrian rhyolites and granites (see: Appendix I). The region surrounding the Precambrian outcrops consists of Paleozoic sedimentary rocks that dip gently way from the Precambrian exposures. The region has been intensely dissected, producing the Ozark hills of southern Missouri. Interfluves correspond to ridges between the various stream valleys. Based on NCIC data for elevations sampled every 65 meters.

Figure 7. Shaded relief image of the NCIC topography shown in Figure 6 with the sun placed 20 degrees above the southern horizon.

Figure 8. Land use map of the Rolla quadrangle. Numbers correspond to the following land use types: 11-residential; 12-17 to urban and industrial areas; 21 to cropland and pasture; 23-24 to agricultural lands; 41 to deciduous forests; 42 to evergreen forests; 43 to mixed forests; 51-52 to streams and lakes; 53 to reservoirs; 61-62 to wetlands; and 76 to transition areas. From USGS Land Use Series Map L-99.

Figure 9. Landsat mosaic for the Rolla quadrangle. Brightness values represent the first principal component values derived from the four channel data. Mosaic from Landsat images 823731-5572500 (30 Jan 76) and 115278-15414 (22 Jan 76).

Figure 10. Contrast enhanced HCMM day IR images centered over the St. Francois Mountains. Data are in a Hotine oblique Mercator projection and are shown in full resolution. The Mississippi River is in the upper right.

Figure 11. Contrast enhanced HCMM night IR images centered over the St. Francois Mountains. Three of the four images show the St. Francois Mountains and interfluvial ridges as bright (warm) anomalies. The lack of contrast in the other scene (June 9) is probably due to atmospheric effects.

Figure 12. Sketch map showing the Missouri gravity low, mapped faults

and folds, and linear features seen in HCMM data. Heavy solid lines indicate the borders of the Missouri gravity low. The dashed line is the glacial till boundary.

Figure 13. HCMM day IR data for the June and September scenes, registered to a Mercator projection and covering the Rolla quadrangle.

Figure 14. HCMM night IR data for the June and September scenes, registered to a Mercator projection and covering the Rolla quadrangle.

Figure 15. Color-coded HCMM images for the Rolla quadrangle, constructed by letting the day IR control the hue, the night IR control the saturation, and the albedo data control the intensity of color associated with any given pixel.

Figure 16. Brightness histograms and color-coding used for Figure 15.

Figure 17. Apparent thermal inertia images for the June and September scenes.

Figure 18,19. National Weather Service meteorological data for the two day-night HCMM pairs covering the Rolla quadrangle. Black dots correspond to the HCMM average temperature for a region covering a 10x10 picture element box centered over Columbia,

Missouri. BEXT is the atmospheric optical depth multiplied by 10,000. Calibration data published in the 1980 HCMM User's Guide were used to convert HCMM data to temperatures.

Figure 20. HCMM day IR (September 29) view centered over the St. Francois Mountains and showing mine tailings piles and residential areas within white box. Box boundaries correspond to the band 4, 5, and 6 Landsat images that are also shown in the figure. Each image is shown at full resolution. Landsat scene 823731-5572500.

TABLE 1

HEAT CAPACITY MAPPING MISSION (HCMM) IMAGE CHARACTERISTICS. FROM HCMM USER'S GUIDE, OCTOBER, 1980.

SPACECRAFT ORBITAL ALTITUDE 620 KM

Circular orbit inclined 97.6° (retrograde) to equator; 1:30 p.m. and 2:30 a.m. crossing, with 16 day repeat cycle

Heat Capacity Mapping Radiometer

Angular resolution	0.83 milliradians
Ground resolution	0.63x0.60 km at nadir (Thermal IR) 0.50x0.50 km at nadir (reflected)
Swath Width	716 km
Thermal channel	10.5 to 12.5 micrometers NEDT = 0.4°K at 280°K
Reflected channel	0.55 to 1.1 micrometers SNR = 10 at 1% reflectance

Note: Radiometric calibration of thermal channel is uncertain. Data may be 5°K lower than true temperature.

TABLE 2

Heat Capacity Mapping Mission (HCMM) data used in analysis of the Ozark region of Southern Missouri. Also shown are meteorological data for roughly same periods for Columbia, Missouri.

DATE (all 1978)	LOCAL TIME	FRAME	CENTER LATITUDE	CENTER LONGITUTDE	TEMP (°K)	WATER VAPOR PRESSURE (mb)	ATMOSPHERIC EXTINCTION COEFFICIENT ($10^{-4} m^{-1}$)
18 MAY	2:30 AM	A-A0022-08200-3	37°32'	90°03'	285	12.62	2.42
9 JUNE	2:30 AM	A-A0044-08310-3	39°02'	93°15'	284	12.59	1.61
10 JUNE	1:30 PM	A-A0045-19420-2	39°02'	93°18'	300	19.25	1.21
14 JUNE	2:30 AM	A-A0049-08250-3	37°00'	92°23'	289	14.17	1.21
19 JUNE	2:30 AM	A-A0054-08180-3	38°14'	90°36'	288	15.85	3.46
16 JULY	2:30 AM	A-A0081-08200-3	39°02'	91°52'	296	26.12	2.42
17 JULY	1:30 PM	A-A0082-19310-2	39°10'	91°53'	305	29.01	3.46
22 AUG	2:30 AM	A-A0118-08060-3	38°23'	89°35'	291	16.09	1.21
2 SEPT	2:30 AM	A-A0129-08120-3	37°29'	91°35'	290	16.27	1.61
29 SEPT	2:30 AM	A-A0156-08160-3	36°32'	93°54'	284	10.50	1.21
29 SEPT	1:30 PM	A-A0156-19090-2	39°20'	88°55'	302	17.22	2.42
15 OCT	2:30 AM	A-A0172-08140-3	36°17'	93°53'	277	7.24	1.21

TABLE 3

Description of Data Used in Analyses of Southern Missouri
Note: HCMM data shown in Table 2.

DATA TYPE	AREAL COVERAGE	DATA DENSITY	RANGE	REFERENCE OF SOURCE DATA
Landsat MSS images	(See Table 4)	79m picture element; 4 channels	128 discrete values for bands 4,5,6;64 for band 7	EROS Data Center, USGS
gamma ray	Rolla quad. 37° to 38°N lat 90° to 92°W long	10km flight line spacing; 67m sample lengths	eU 0-8.3ppm eTh 0-16.9ppm K 0-4.7%	DOE-NURE (Texas Inst., 1979)
topography	Continental United States	average elevations every 1km	-----	NCIC, USGS
topography	Rolla quad.	average elevations every 63.5m	99-540m	NCIC, USGS
stream sediment elemental abundances	Rolla quad.	700 samples 0.037 samples/km2	elements: Na,Al,Sc, Ti,V,Mn, Fe,Hf,Ce Th,U (done via Neutron Activation Analysis)	DOE-NURE (Fay et al., 1982)
gravitational anomalies	Continental United States	25,656 stations 0.162 station/km2	-72 to 37 mgals	DMAAC
aeromagnetic total field intensity amonalies	36° to 38°N lat 90° to 92°W long	10km flight line spacing; 67m sample lengths	-1700 to 500 gamma	DOE-NURE (Texas Inst., 1979)

TABLE 4

Landsat Multispectral Scanner Frames Used in Data Analysis.
The January 22nd and 30th scenes were digitally mosaicked for the 1°x2° Rolla Quadrangle.

DATE	SCENE I.D.	CENTER LAT.	CENTER LON.	SUN ELEVATION ANGLE	SUN AZIMUTH ANGLE (CW FROM NORTH)
January 3, 1976	11259-15365	38°48'	89°53'	19°	144°
January 5, 1976	11261-15483	37°23'	93°13'	20°	143°
January 22, 1976	11278-15414	37°24'	91°50'	21°	140°
January 22, 1976	11278-15412	38°49'	91°22'	21°	140°
January 29, 1976	20372-15514	37°22'	88°56'	25°	143°
January 30, 1976	823731-5572500	37°19'	90°23'	26°	143°

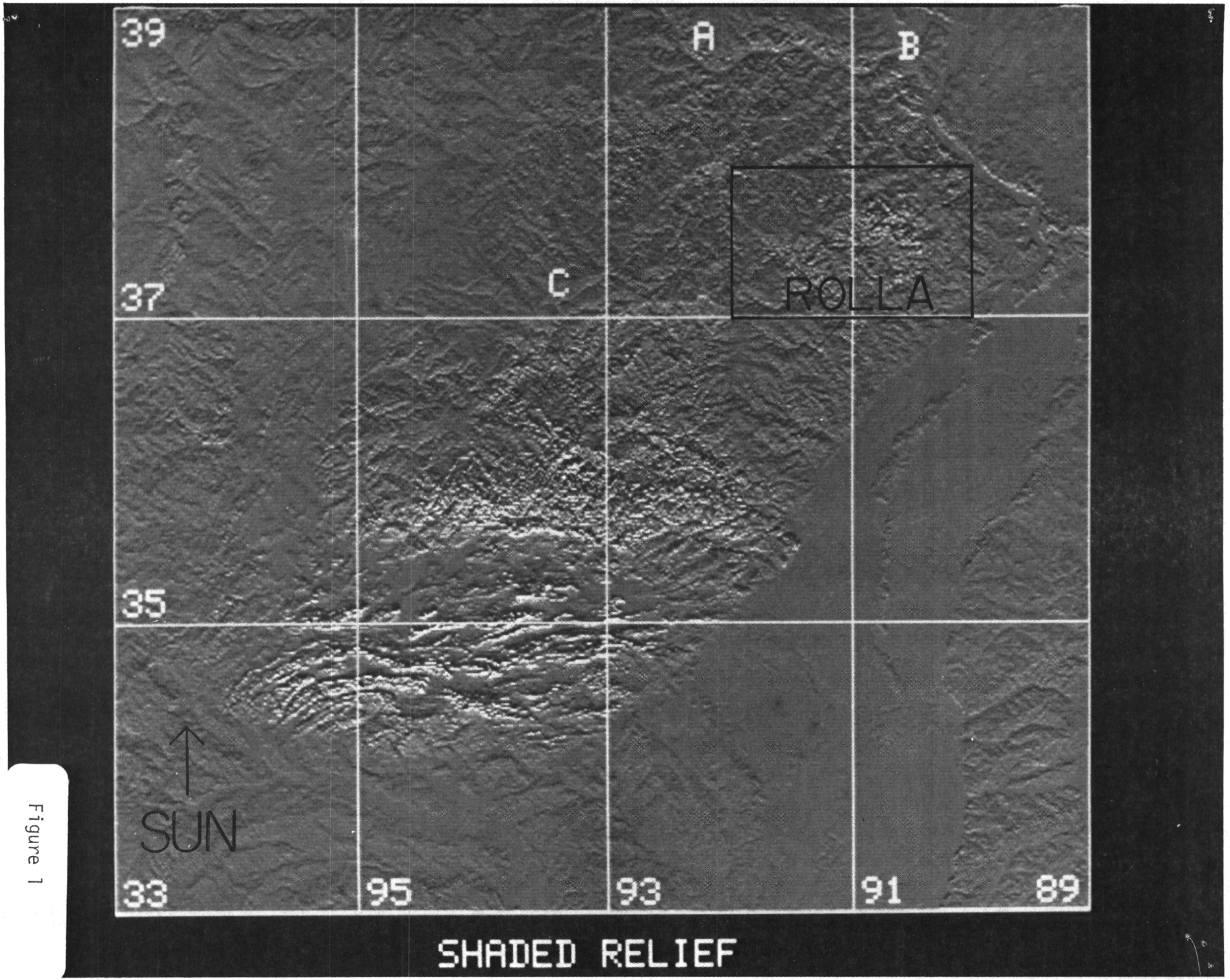

Figure 1

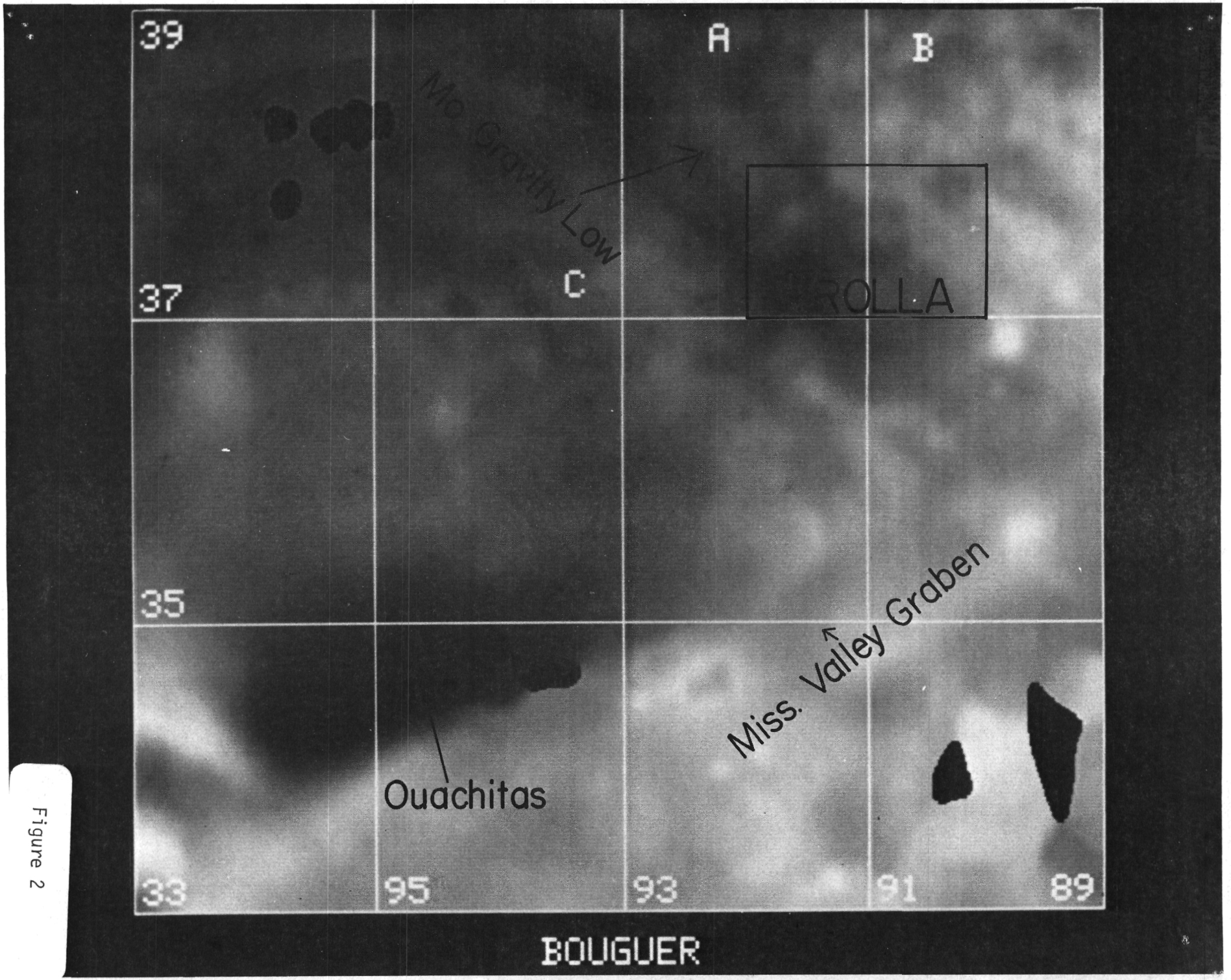
39
A
B
Mo Gravity Low
37
C
ROLLA
35
Miss. Valley Graben
Ouachitas
33
95
93
91
89
BOUGUER

Figure 2

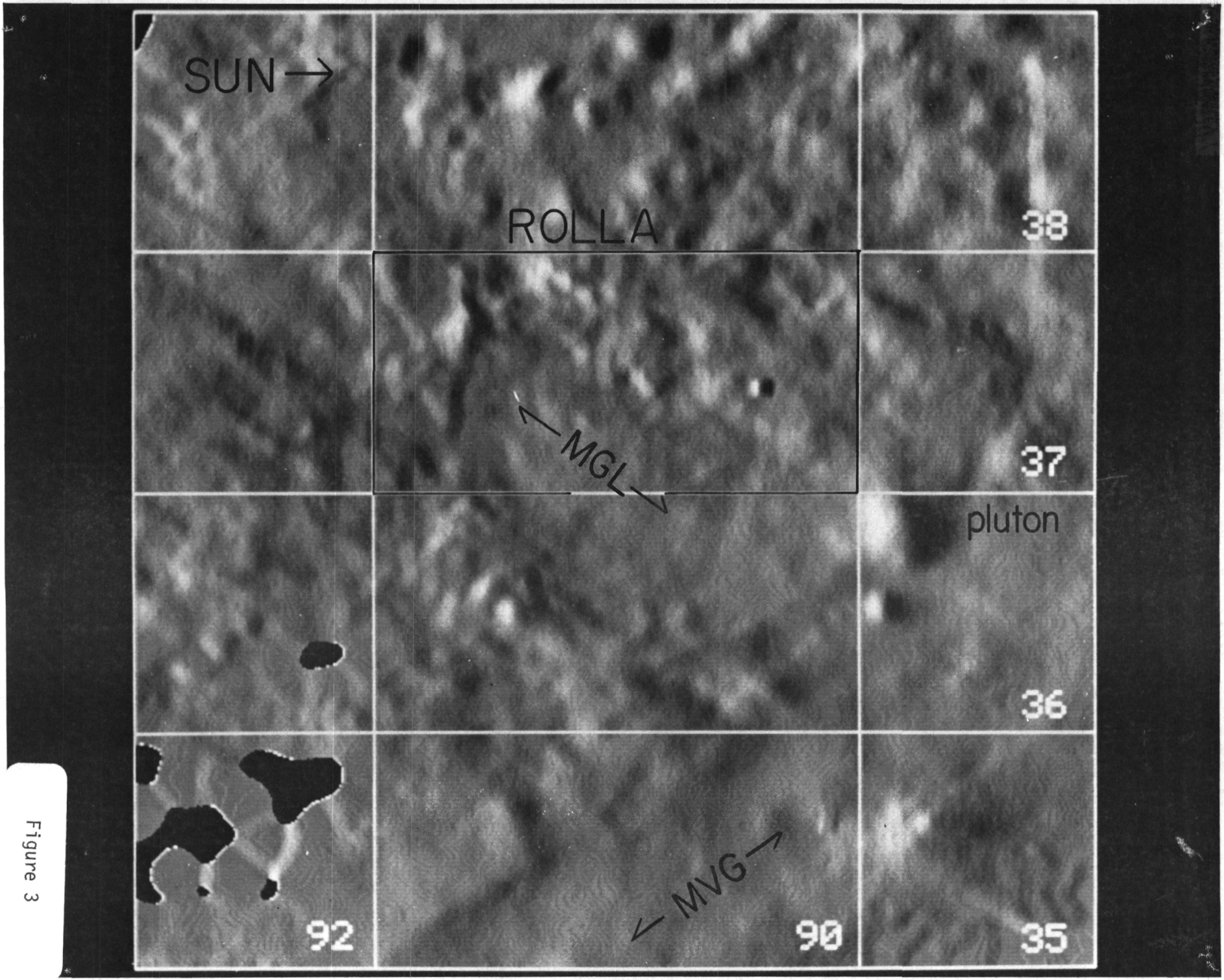

Figure 3

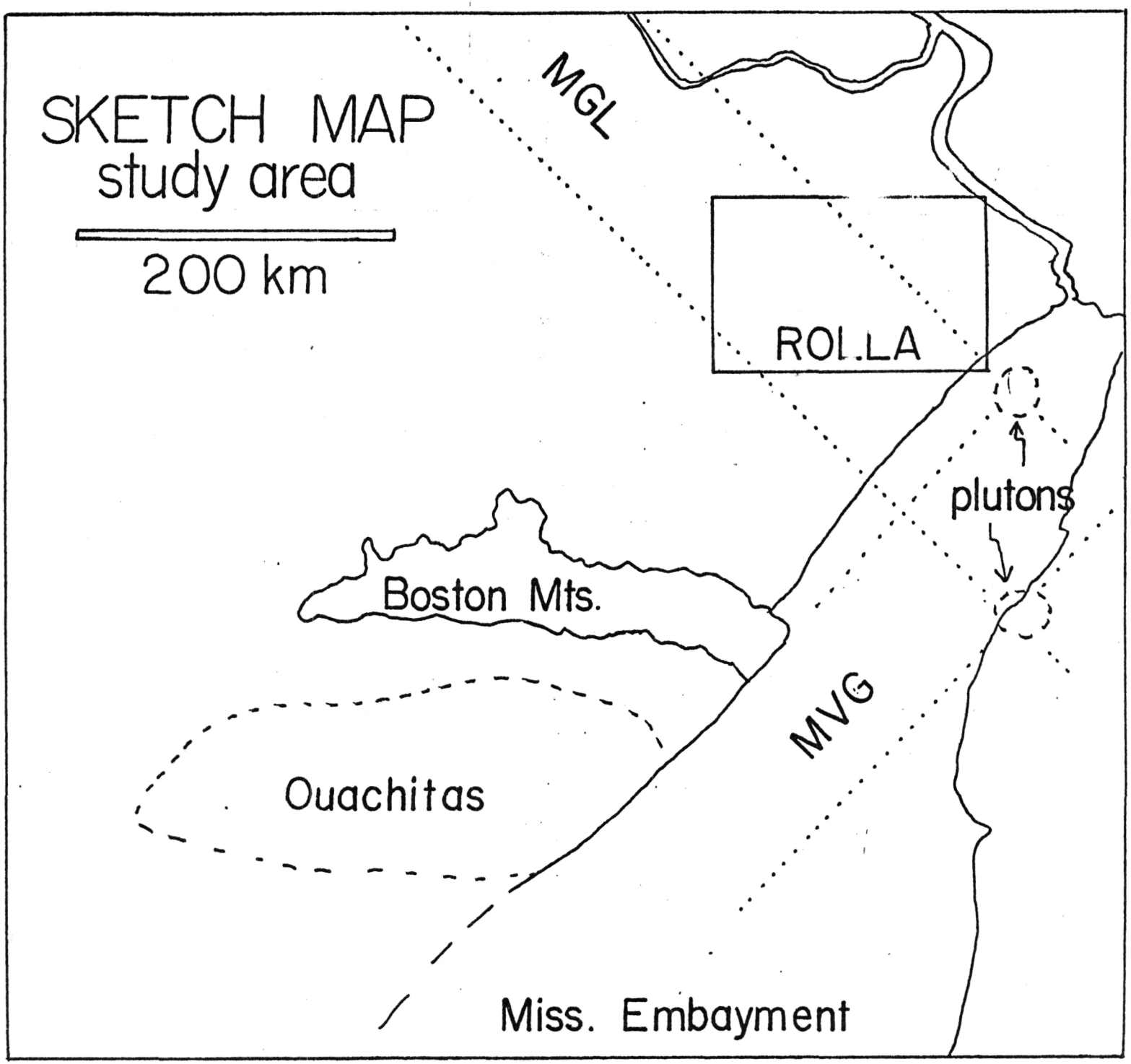
SKETCH MAP
study area
200 km
MGL
ROLLA
plutons
Boston Mts.
MVG
Ouachitas
Miss. Embayment

Figure 4

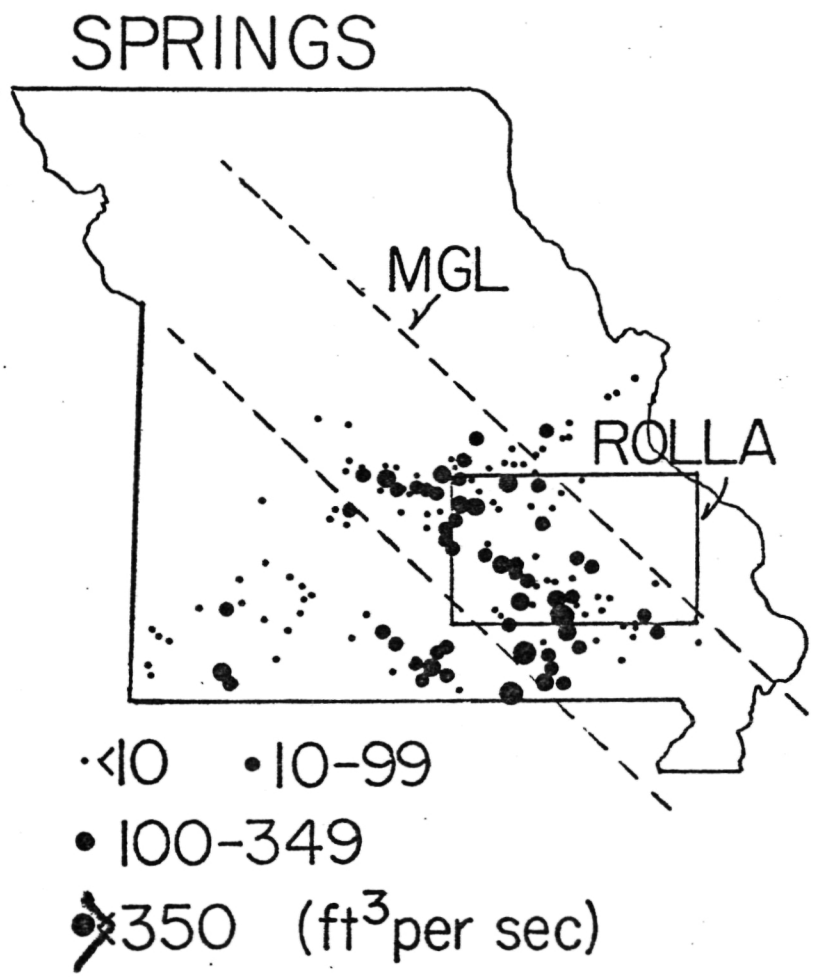

Figure 5

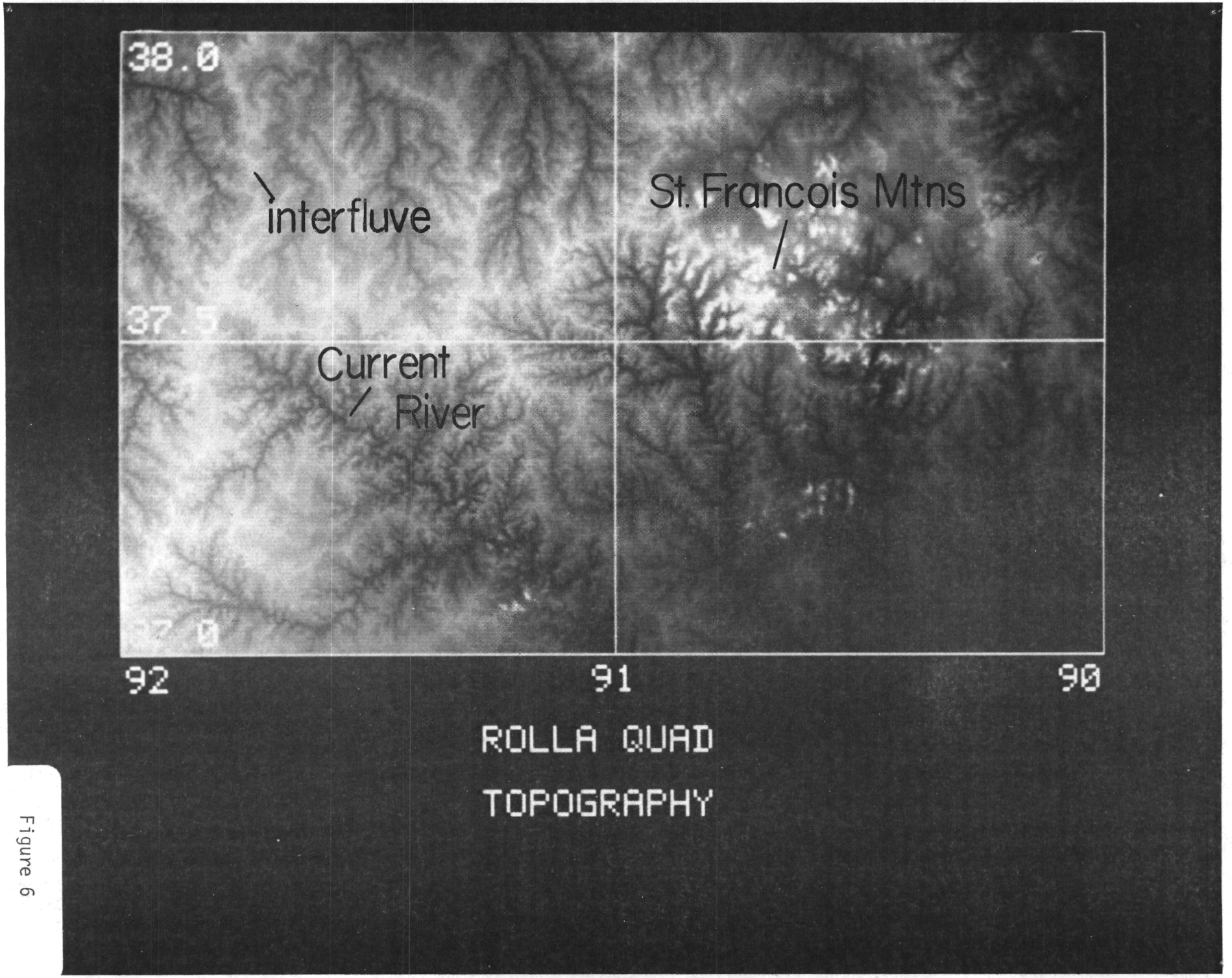
38.0
interfluve
St. Francois Mtns
37.5
Current
River
92
91
90
ROLLA QUAD
TOPOGRAPHY

Figure 6

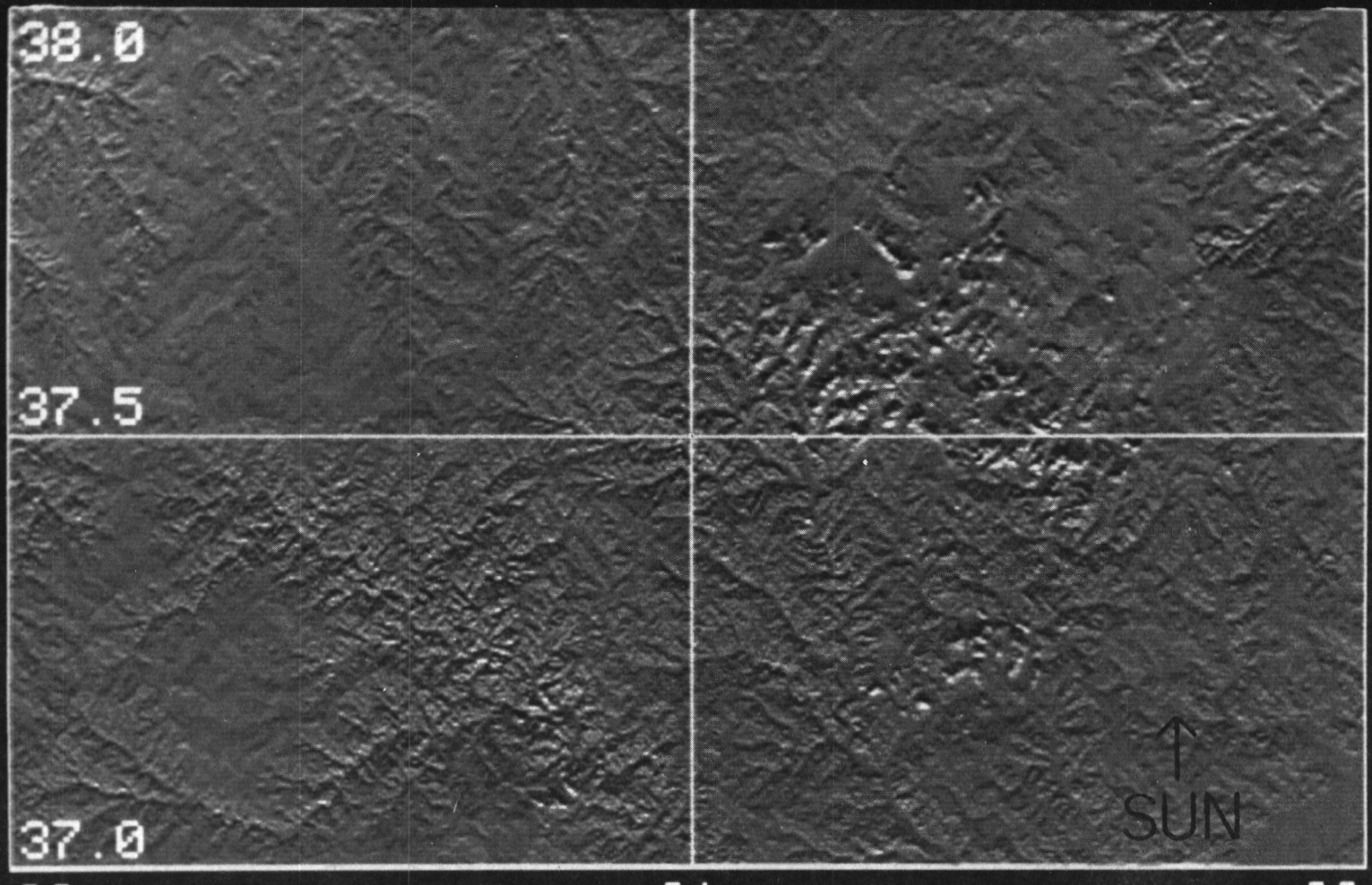

ROLLA QUAD

SHADED RELIEF

Figure 7

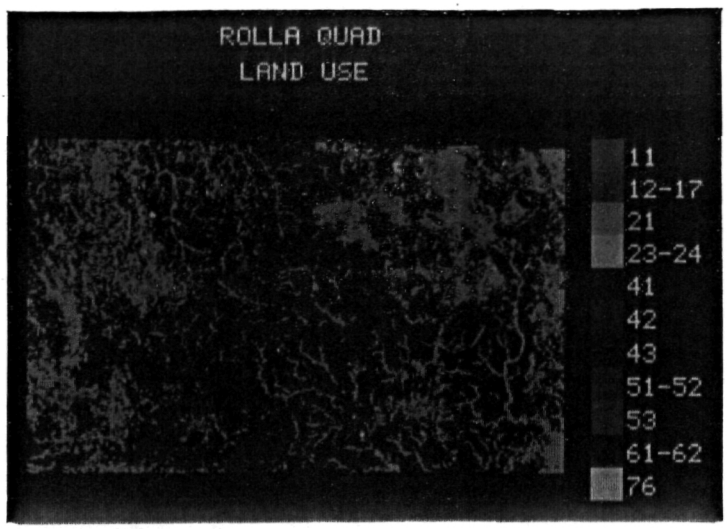

Figure 8

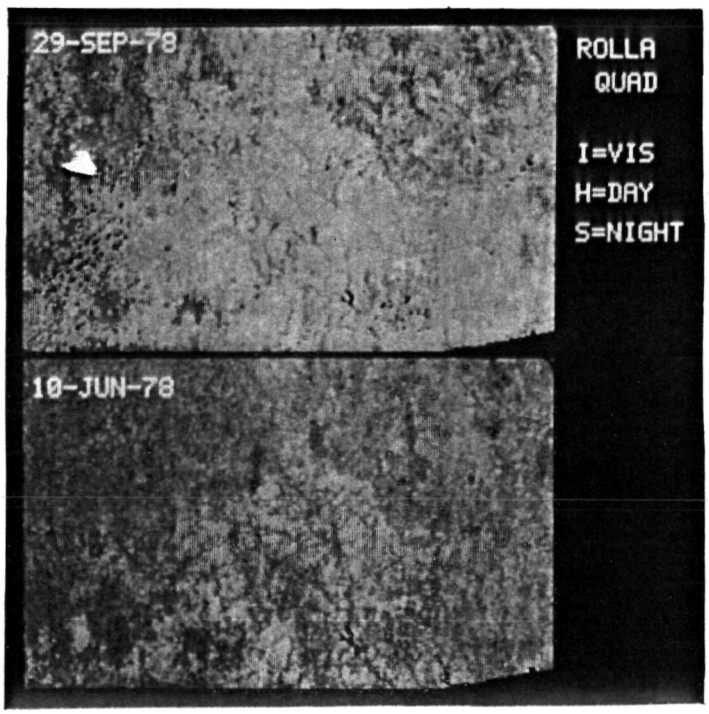

Figure 15

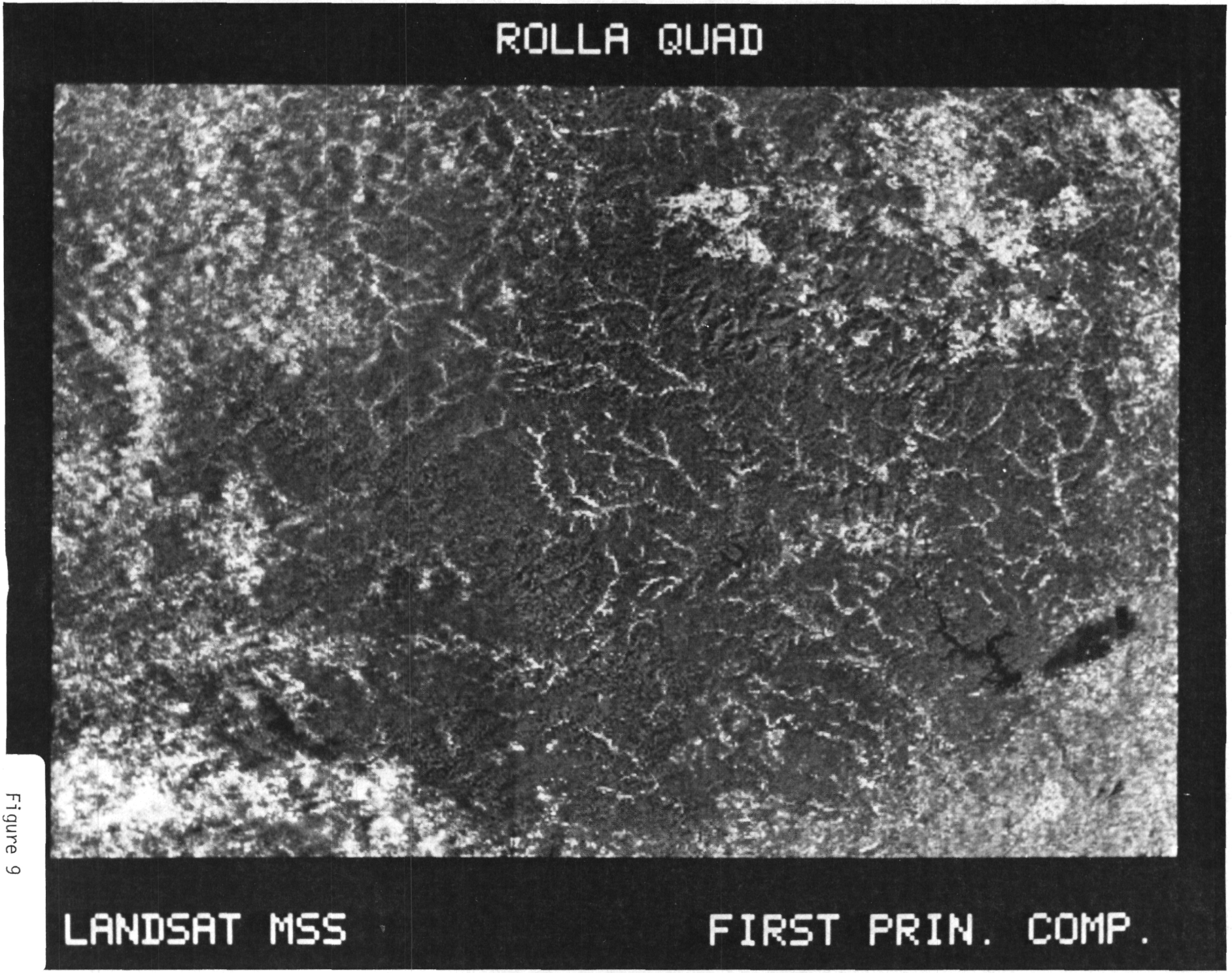

Figure 9

Figure 10

Figure 11

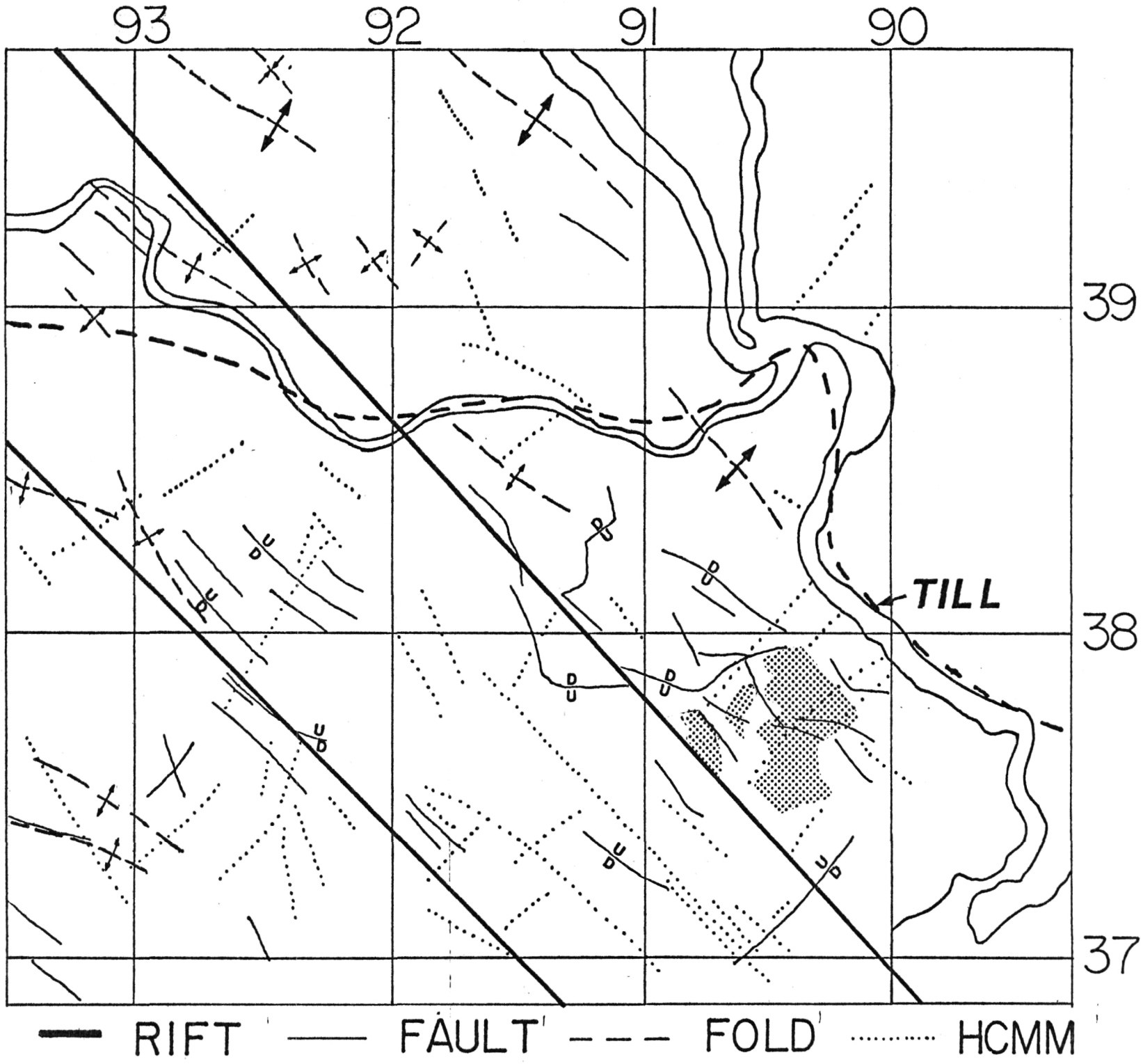

Figure 12

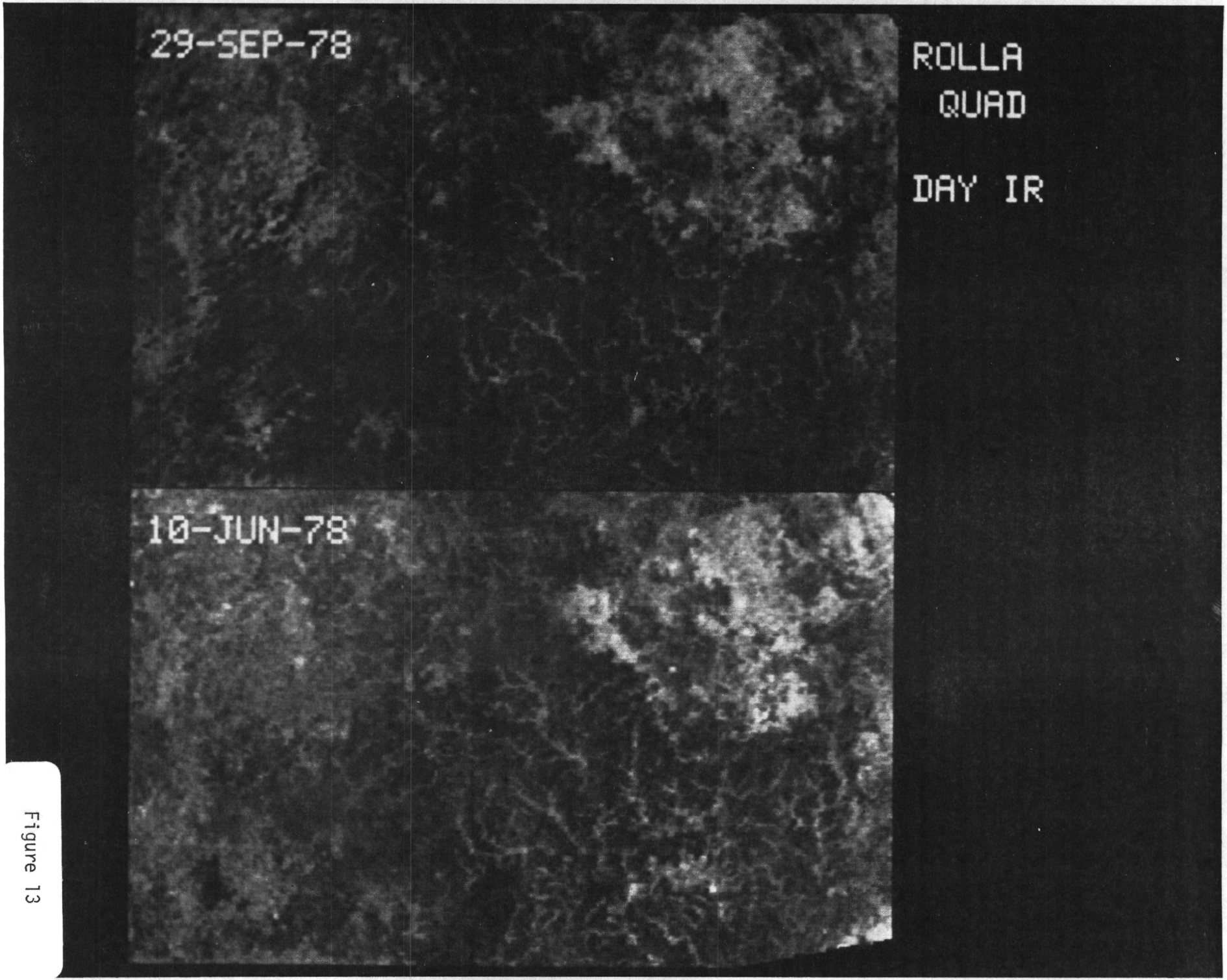

Figure 13

Figure 14

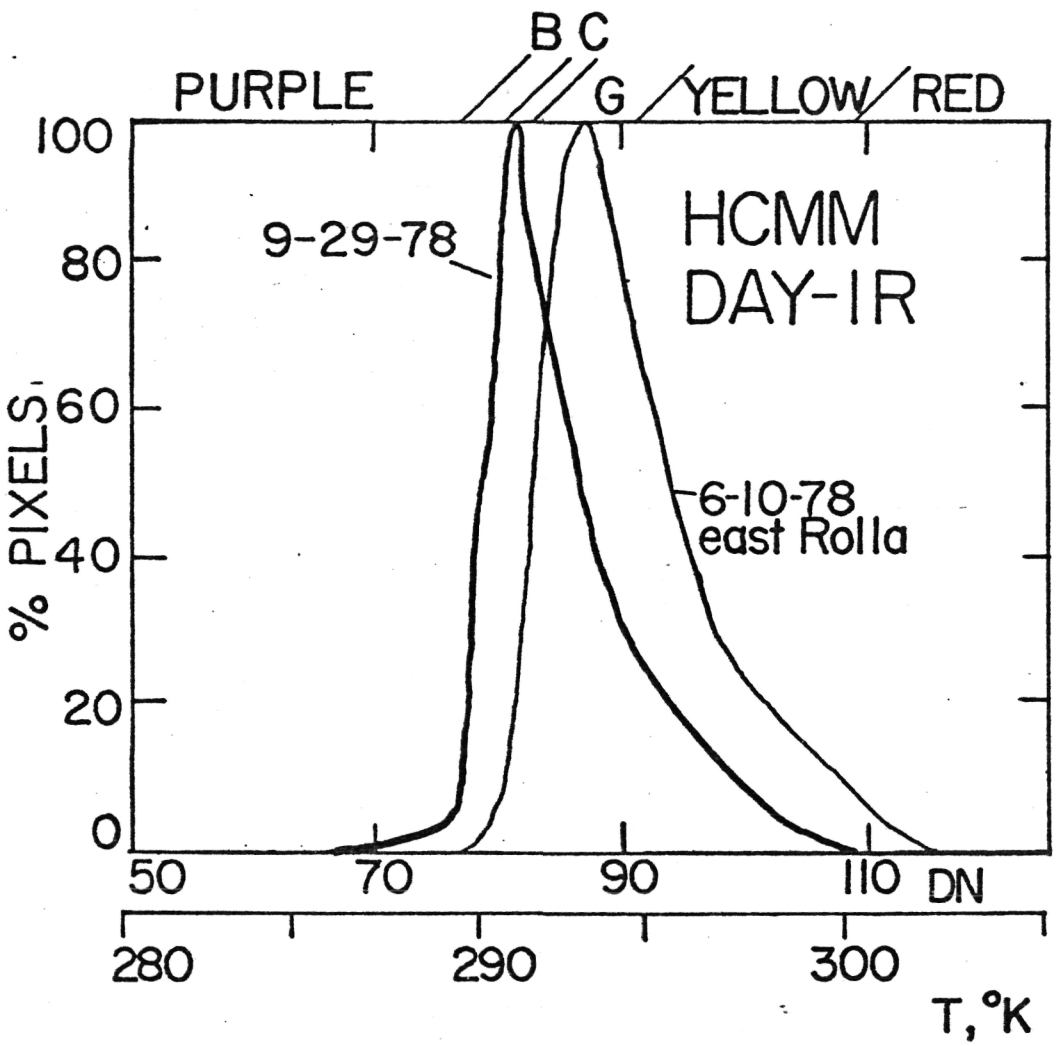
B C
PURPLE
G
YELLOW
RED
100
80
60
40
20
0
% PIXELS
9-29-78
HCMM
DAY-1R
6-10-78
east Rolla
50
70
90
110
DN
280
290
300
T, °K

Figure 16

Figure 17

Figure 18

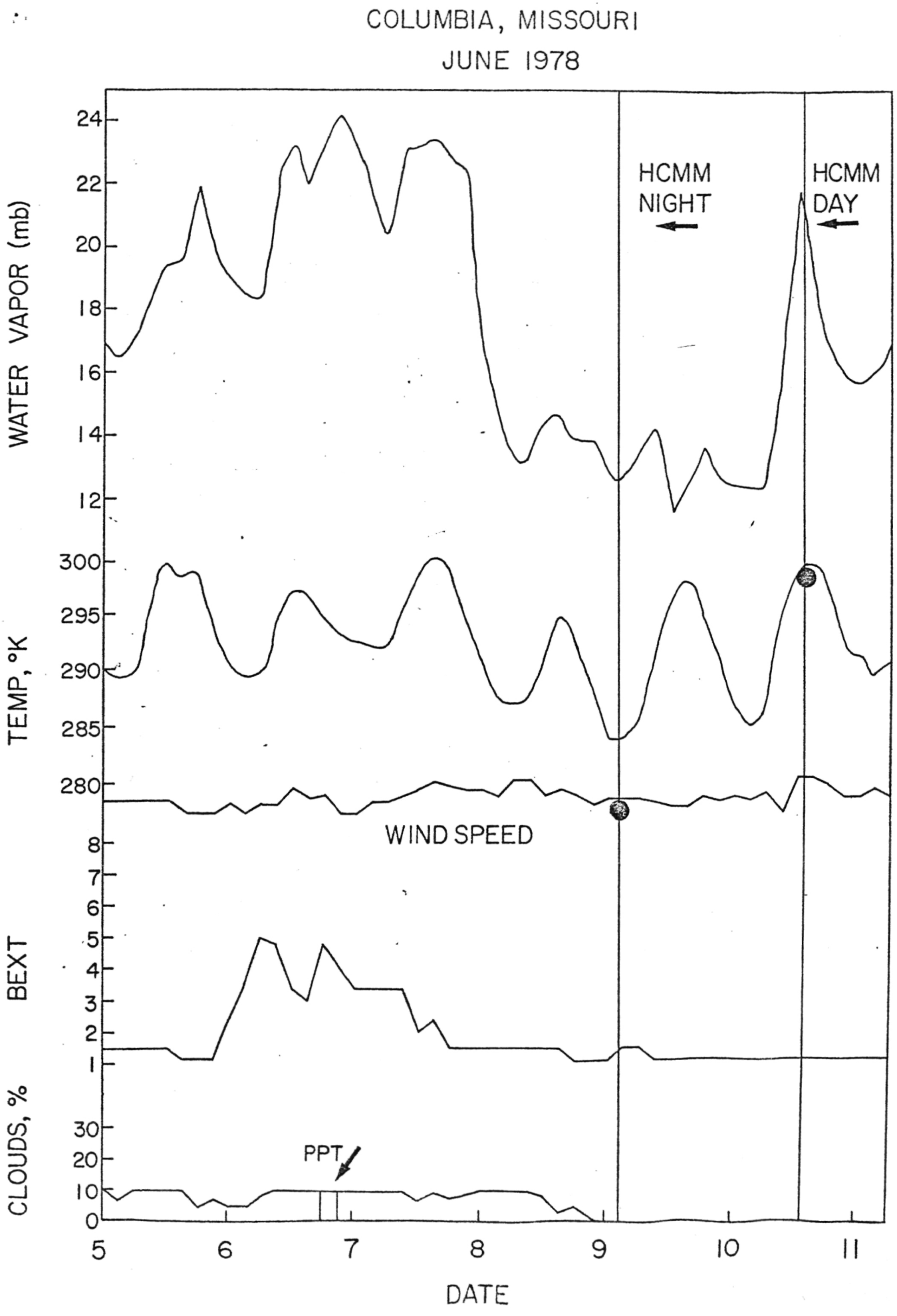
COLUMBIA, MISSOURI
JUNE 1978
WATER VAPOR (mb)
24
22
20
18
16
14
12
HCMM NIGHT
HCMM DAY
TEMP, °K
300
295
290
285
280
WIND SPEED
8
7
6
5
4
3
2
1
BEXT
CLOUDS, %
30
20
10
0
PPT
5
6
7
8
9
10
11
DATE

COLUMBIA, MISSOURI
SEPTEMBER 1978

Figure 19

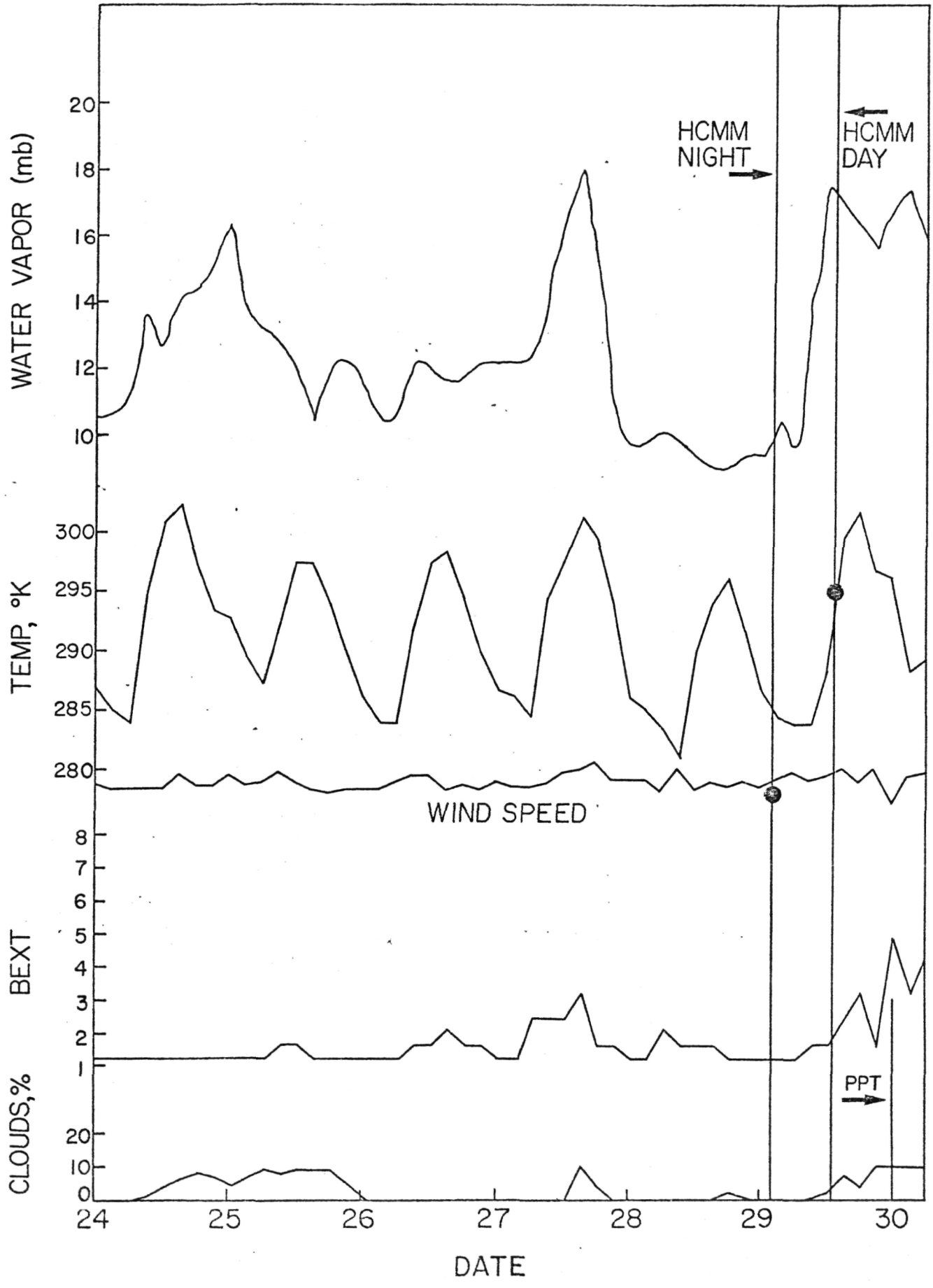

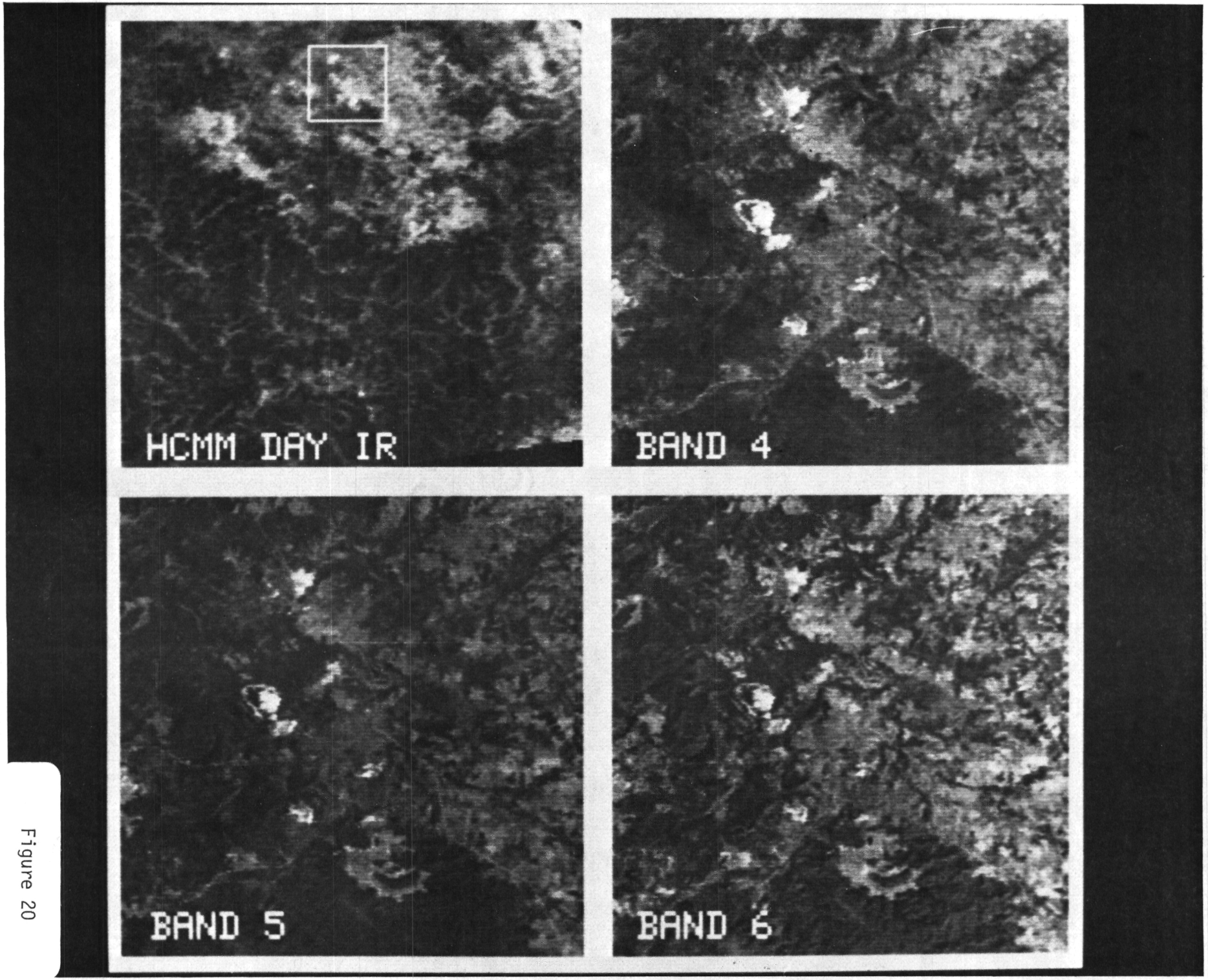

Figure 20

JOURNAL OF GEOPHYSICAL RESEARCH, VOL. 87, NO. B10, PAGES 8529–8545, OCTOBER 10, 1982

Identification of a Precambrian Rift Through Missouri by Digital Image Processing of Geophysical and Geological Data

E. A. GUINNESS, R. E. ARVIDSON, J. W. STREBECK, K. J. SCHULZ, G. F. DAVIES, and C. E. LEFF

Department of Earth and Planetary Sciences, McDonnell Center for the Space Sciences, Washington University St. Louis, Missouri 63130

Digital free air and Bouguer gravity anomaly images have been constructed from approximately 287,000 station readings for the region bordered by 25°–49°N latitude and 80°–110°W longitude. The technique used to interpolate between station locations was based on a two-dimensional spatial filter, where the average of the anomaly values located within the filter area was computed. The images contain as many as 256 contours (values in byte variable), so that subtle anomaly patterns can be identified and traced with much greater certainty than on most contour maps. A newly discovered feature in the midcontinent is a gravity low that begins at a break in the midcontinent gravity high in SE Nebraska, extends across Missouri in a NW-SE direction, and intersects the Mississippi Valley graben to form the Pascola arch. The anomaly varies from 120 to 160 km in width, extends about 700 km, and is best expressed in southern Missouri, where it has a Bouguer amplitude of approximately −34 mGal. The magnitude of the anomaly cannot be explained on the basis of a thickened section of Paleozoic sedimentary rock. The gravity data and the sparse seismic refraction data for the region are consistent with an increased crustal thickness beneath the gravity low. Some of the discrete positive magnetic anomalies in Missouri are located along the borders of the gravity low. Digitally enhanced thermal infrared images from the Heat Capacity Mapping Mission show a distinct alignment of linear structures with the gravity feature. The linear features in some cases correspond to mapped high-angle normal faults, to drape folds over relief within the Precambrian basement, and in some cases to extensions of mapped structures. The gravity anomaly also cuts across the major Precambrian boundary in SE Missouri, marking the change from older, sheared granites and metasedimentary rocks to younger granites and rhyolites. Given the cumulative evidence, the gravity anomaly is probably the present expression of a failed arm of a rifting event, perhaps one associated with the spreading that led to or preceded formation of the granite and rhyolite terrain of southern Missouri.

INTRODUCTION

We have been pursuing relationships between the pattern, age, and origin of structural features within the Precambrian basement rocks of southern Missouri and the locations and genesis of ore deposits. The area is a well-known lead mining district, where Mississippi Valley type Pb-Zn-Cu ores have accumulated in Cambrian carbonate rocks associated with stromatolitic reef and back-reef facies [*Gerdemann and Meyers*, 1972]. The location of these facies was controlled by the location of the shoreline, which was in turn controlled by the pattern of faulting of the Precambrian basement [*Grundmann*, 1977; *Sweeney et al.*, 1977; *Evans*, 1977; *Paarlberg and Evans*, 1977; *Mouat and Clendenin*, 1977]. In addition, iron ores of magmatic origin can be found in the Precambrian basement rocks along fracture zones [*Kisvarsanyi*, 1976].

Structural studies of basement rocks in southern Missouri have been pursued for a considerable amount of time [see *Kisvarsanyi and Kisvarsanyi*, 1976], and a significant amount of information has been gained on the distribution of Precambrian rock types and ages [*Kisvarsanyi*, 1974; *Bickford et al.*, 1981; *VanSchmus and Bickford*, 1981]. However, little has been done in terms of understanding how the structure of the region is related to the overall structural configuration of the midcontinent or how such features are related to the structural history of the area. In this paper we utilize digital image-processing techniques to reduce and display a variety of potential field, topographic, geologic, and remote sensing data for the midcontinent. The intent is to delineate how structural patterns in southern Missouri are related to the broader features of the midcontinent.

Paper number 2B1045.
0148-0227/82/002B-1045$05.00

DESCRIPTION OF DATA AND PROCESSING METHODS

Digital image-processing techniques have a potentially wide range of utility for display and analysis of geographically (i.e., array) oriented data sets. In our case, data covering the midcontinent were processed on a PDP-11/34 minicomputer with interactive image display peripherals, using standard digital image enhancement, filtering, and geometric operations. The reader is referred to standard texts such as that by *Moik* [1980] for further information on image-processing techniques and to *Arvidson et al.* [1982] for examples of the utility of image processing in processing, display, and interpretation of topographic and gravity data for the continental United States.

National Oceanic and Atmospheric Administration digital topography, together with land station measurements of gravitational acceleration, comprise two important data sets that we employed in the study. The area chosen for analysis of the topography and gravity ranges from 25° to 49°N latitude and from 80° to 110°W longitude, thereby covering regions from the eastern edge of the Rocky Mountains on the west to the Appalachians on the east and from the Superior Province on the north to the Gulf of Mexico on the south. The topography consists of average elevations for areas covering 30″ in both latitude and longitude. Gravity stations are typically spaced 3 km apart but vary between hundreds of meters to 10 km over the study area. The gravity data were reduced to free air and to Bouguer anomalies courtesy of the Defense Mapping Aerospace Agency Center, St. Louis, Missouri. The reference field at sea level used was

based on the 1967 International Gravity Formula, with all the data referenced to the 1971 International Gravity Standardization Net. Bouguer anomalies were computed on the basis of a slab model with a density of 2.67 g/cm^3. No local terrain corrections were included.

Magnetic anomalies were also included in the analysis. Unfortunately, digital data for the region were not available at a reasonable cost. Consequently, we restricted inclusion of magnetic coverage to the state of Missouri, based on the 1943 statewide contour map of vertical field intensity anomalies. The 1943 map was checked against a new, unpublished map by I. Zietz, and both maps were found to exhibit similar trends. The 1943 map was photographed onto film, and the film was then scanned and digitized, resulting in a digital image of magnetic anomaly contours for Missouri. Similarly, the basement rock type map for the midcontinent compiled by *Bickford et al.* [1981] and *VanSchmus and Bickford* [1981] was transformed to a digital format for use in comparison with other data sets.

Other digital data sets that were utilized in this work included Heat Capacity Mapping Mission (HCMM) images. HCMM consisted of a satellite with sensors capable of imaging the surface in the visible to the reflected infrared (one channel covering 0.5–1.1 μm) and in the thermal infrared (one channel from 10.5 to 12.5 μm) [*Price*, 1977]. Each image element in the HCMM data covers about 500 m

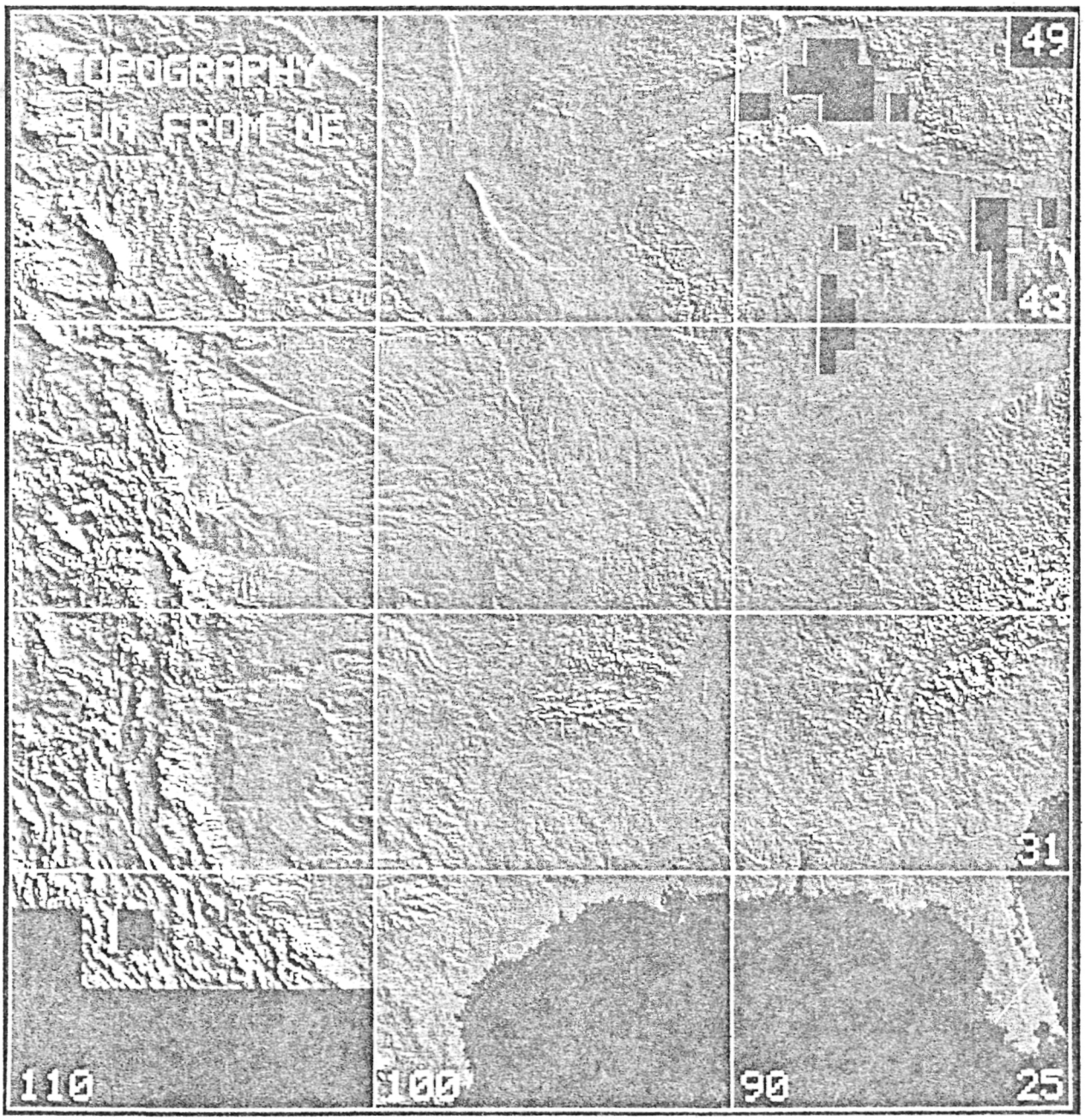

Fig. 1. Digital shaded relief map of topography displayed in this image with the simulated sun located at 20° above the northeastern horizon. A Mercator projection is used for this image and the other images in the paper. Numbers running vertically on the right-hand side are degrees north latitude, and numbers at the bottom are degrees west longitude. The particular area of concern is located in the box bounded by 25°–49°N latitude and 80°–110°W longitude. The resolution of the image, measured as the width of a picture element (pixel) is about 7 km. At that resolution, little structural control of topography is evident with the midcontinent.

across, and one scene covers about 700 km in width and in height. The visible–reflected infrared sensor was used to measure the broadband albedo of the surface, while thermal infrared data acquired during the day and night provided information on the magnitude of diurnal temperature changes. These parameters can be used to solve for the thermal inertia of the surface, a thermophysical property that depends on the density, thermal conductivity, and specific heat [*Kahle et al.*, 1976]. Thermal infrared data, including estimates of thermal inertia, have been shown to be useful in delineating structural features in a variety of geological contexts [*Sabins*, 1969; *Offield*, 1975; *Watson*, 1981]. HCMM data were included in this study both because of the applicability of thermal data in structural studies and because the synoptic view is appropriate for examining the surface expression of regional-scale structures. HCMM images for southern Missouri were contrast-enhanced, digitally registered to one another, and displayed in a variety of formats designed to emphasize structural trends. Details of HCMM processing techniques will be discussed in a later section.

The first step in the analysis of topographic and gravity data was to scale the dynamic range of the data to fit within the range of a byte variable (i.e., 8 bits or 256 discrete values). The byte data were then stored in image arrays, registered to a common base if needed, and processed. Final displays were transformed to Mercator projections and overlaid with latitude-longitude grids. The byte-encoded topographic data were first stored in an array with 30″ spacing in both latitude and longitude. The data could be displayed as an image if the byte-encoded values were converted to brightness or to color values. Alternatively, a shaded relief image could be constructed if a photometric function for the surface is assumed. Figure 1 shows a shaded relief image transformed to a Mercator projection and depicting topography under the assumption that the surface obeys the Lommel-Seeliger scattering law [*Batson et al.*, 1975]. The simulated sun is from the northeast at 20° above the horizon.

Generation of images from the gravity anomaly values is more complicated than generating displays from the topographic data. The reason is that the gravity stations are not located along regular grid intersections. We chose a simple but powerful spatial filtering technique for interpolating between station locations. The byte-encoded anomaly values were first assigned to array locations closest to the station locations. This procedure produced an array in part occupied by valid data and in part occupied by blank zones. The filtering algorithm that we then applied was developed by *Eliason and Soderblom* [1977], used to produce topographic maps from the Pioneer Venus altimetry data [*Pettengill et al.*, 1980] and applied to generating gravity images for the continental United States by *Arvidson et al.* [1982]. The technique involves use of a spatial filter of $N \times N$ elements. The average of the valid data points within any given filter location is computed and used to replace the center value, but only if a valid datum does not already exist at that array location. In practice, the gravity data were processed using several filter passes, beginning with a 3×3 element filter and ending with a 21×21 element filter. The choice of filter sizes was governed by station spacings, which varied from hundreds of meters to 10 km. The result is an interpolated data set, except for regions that had so few valid data points that a user-defined threshold was not met. In our case we set the threshold so that at least 20% of the elements for any filter position would have to have been occupied by valid data for an interpolation calculation to proceed.

The interpolated gravity data can be displayed as a gray tone image, as is done in Figure 2 for free air anomalies. Black areas in the image correspond to zones with too few stations to allow valid interpolations. The gravity data can also be displayed as a shaded relief image, where gravity highs and lows are illuminated as if they were hills and valleys. Figure 3 is a shaded relief image of the free air anomalies with the simulated sun placed at 15° above the northeastern horizon.

The gravity anomaly images displayed in Figures 2 and 3 and equivalent Bouguer anomaly presentations have been checked against published maps [e.g., *Woollard and Joesting*, 1964; *McGinnis et al.*, 1979; *Simpson and Godson*, 1981]. Generally, the images and published maps correspond. However, the images have intrinsically more information displayed, for at least three reasons. First, the grid spacing used to interpolate between station readings is more closely spaced than the spacing used to generate most published continent-wide contour maps. Second, there can be as many contour intervals in our displays are there are values in a byte (256). Third, because of the particular filtering algorithm used, areas with closely spaced stations retain local details of anomaly patterns. For instance, Figures 2 and 3 show a major gravity feature (free air low) that begins at a break in the midcontinent gravity high and extends about 700 km to the southeast. One of the distinguishing aspects of this feature is not the amplitude of the low but rather the sharp gravity gradient associated with the edges of the anomaly. Although sections of the feature have been noted in the past [see *Phelan*, 1969; *Cordell*, 1979; *Russ*, 1981], the images shown in Figures 2 and 3 provide new information and a broader perspective that show the entire trend and location much more accurately than can be seen in published maps.

Finally, an important aspect of comparing data sets is the ability to merge or overlay one data set onto another to produce a visual display that maximizes the eye's ability to see correlations between the data sets. A useful technique is to allow one data set (gravity anomalies, for instance) to control the hue (dominant wavelength) and saturation (degree of purity) of a color image, while another data set (topography, for instance) controls the color brightness [*Arvidson et al.*, 1982]. Also, it is possible to combine values of a given parameter with a shaded relief presentation of that parameter by allowing the value to control the color hue and saturation, while the local gradient, expressed in shaded relief form, controls the brightness [*Pettengill et al.*, 1980; *Kobrick*, 1982]. For example, Plate 1 is a version of the Bouguer image where the values have been color-coded and overlain onto a shaded relief version of the anomalies. The effect is to produce an enhancement showing information related both to the value of the anomaly and to the local gravity gradient.

Basement Structure in Missouri as Defined by Gravity Anomalies and Seismic Profiles

Figure 4 is a sketch map showing some of the major structural features seen in the free air anomaly images shown in Figures 2 and 3 and in the Bouguer image shown in Plate 1.

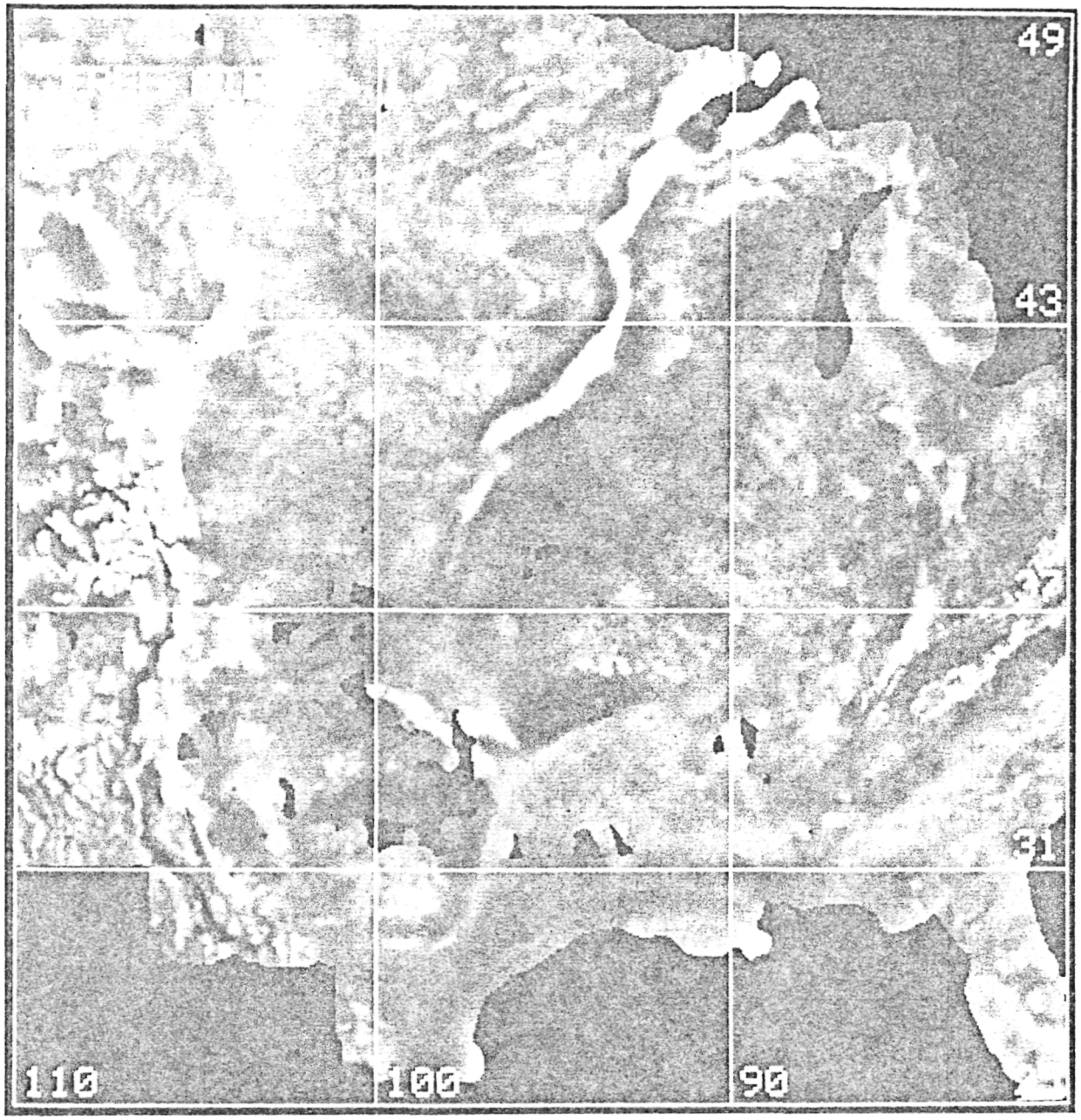

Fig. 2. Gray tone image of free air gravity anomalies for the same area as displayed in Figure 1. Black areas correspond to regions where stations were spaced too far apart to allow reasonable interpolation. Bright regions correspond to positive anomalies, medium gray to areas with anomalies close to zero, and darker areas to regions with negative anomalies. The anomaly range goes from +66 to −360 mGal. A sketch map illustrating structural features evident in the image is shown in Figure 4. The midcontinent gravity high extends as a NE-SW trending linear high, flanked by lows, in the upper half of the image. Note the subtle linear low extending from a break in the gravity high, toward the southeast, to about 36°N latitude, 90°W longitude.

The midcontinent gravity high is a major gravity anomaly in the midcontinent. In our data this feature has a maximum free air anomaly of 85 mGal and a maximum Bouguer anomaly of 50 mGal. The midcontinent gravity high is about 70 km wide, contains Keweenawan basalts that date at 1.1 b.y., and has been interpreted as a failed continental rift [*Chase and Gilmer*, 1973]. Flanking lows on either side of the high have been modeled as thick (several kilometers) arkosic sediments deposited as the load associated with the basalts caused regional subsidence. Considerable structure can also be seen in the greenstone-granitic terrain of the Superior Province located to the northwest of the midcontinent gravity high. The Wisconsin arch, the Ouachitas, and the Wichita-Arbuckle system are just a few of the other features that have a recognizable gravity signature. For reference, the Ouachitas have minimum free air and Bouguer anomalies of −70 and −89 mGal.

A subtle but pervasive gravity feature seen in both the free air and the Bouguer images is a linear low that begins at a break near the southeastern end of the midcontinent gravity high (40.5°N latitude, 96°W longitude), strikes in a southeasterly direction, and extends to the Mississippi Valley graben as defined by *Kane et al.* [1981] (36°N latitude, 90°W longitude). The low varies between 120 and about 160 km in

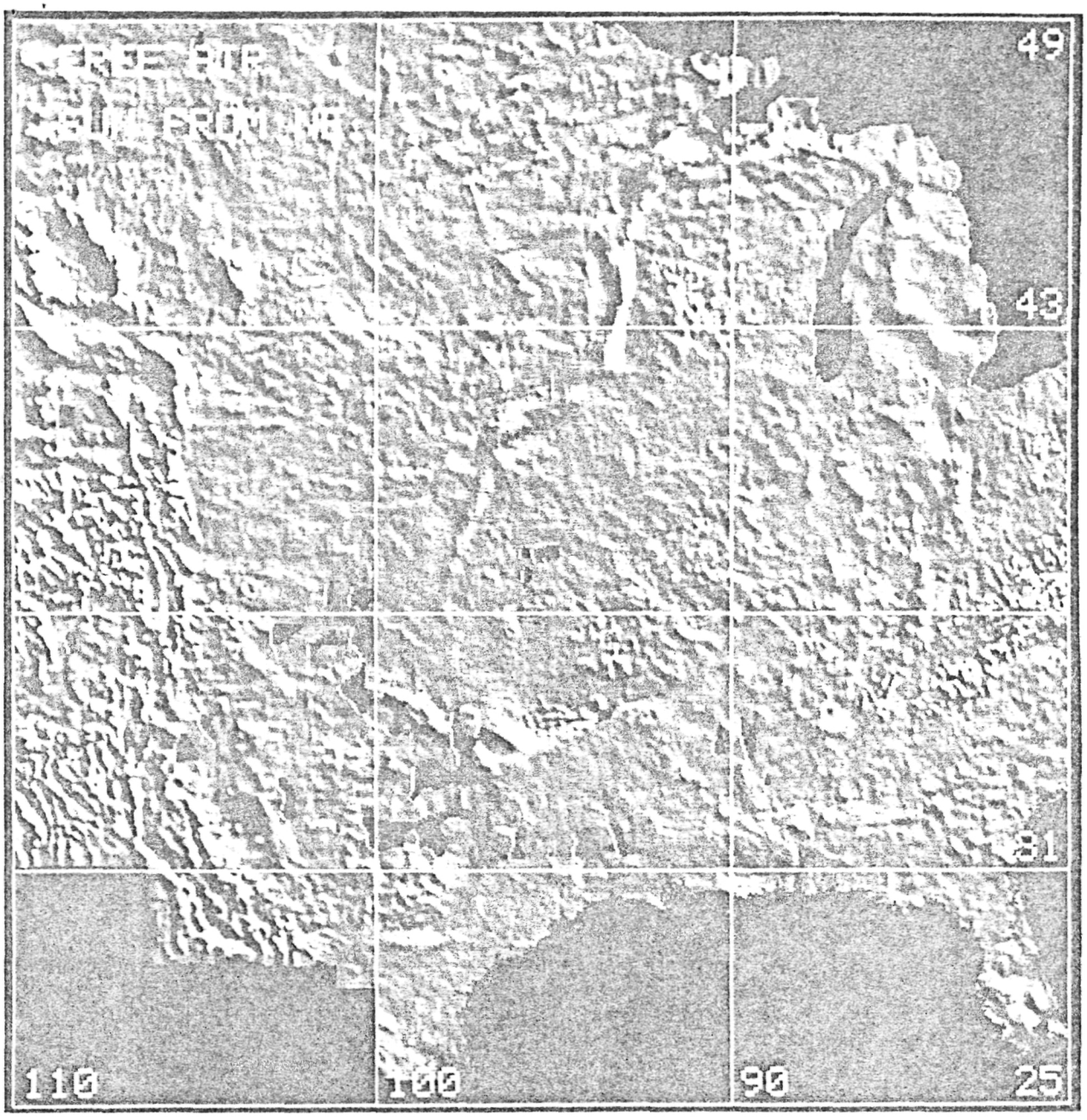

Fig. 3. Shaded relief image depicting free air anomalies as if they were hills and valleys illuminated by a sun located at 15° above the northeastern horizon. Note the correlation between the shaded relief of topography and this figure in areas of high relief. Also note the linear gravity low that begins at the break in the midcontinent gravity high and strikes southeasterly toward 36°N latitude, 90°W longitude. A Bouguer image displays a similar pattern for the linear gravity low.

width, extends about 700 km in length, and is best expressed for the 300 km of its length closest to the graben. The feature also exhibits an irregular medial high (Figure 3) midway between the midcontinent gravity high and the graben. The feature begins just to the northwest of Missouri and ends just beyond the southeastern boundary of the state. We therefore informally refer to the feature as the Missouri gravity low. As discussed by *Arvidson et al.* [1982], the intersection of the Missouri gravity low with the Mississippi Valley graben is the site of the majority of the microseismic epicenters recorded in the 1970's by the St. Louis University seismic network [*Stauder et al.*, 1977]. In addition, the northern boundary of the intersection is the site of the circular Bloomfield anomaly, while the southern boundary is the site of the Covington anomaly. Both features can be seen in the free air and Bouguer data as distinct, circular positive anomalies. *Kane et al.* [1981] suggest that these two anomalies, which are also positive magnetic anomalies, are due to intrusions of magmas during the Mesozoic era. The intersection of the Missouri gravity low and the Mississippi Valley graben is also the site of the Pascola arch as defined by *Phelan* [1969] and *Ervin and McGinnis* [1975].

Several gravity profiles were generated across the Missouri gravity low to illustrate its form and to model subsurface density configurations. The location of the southernmost profile is shown in the sketch map in Figure 4. Values for the

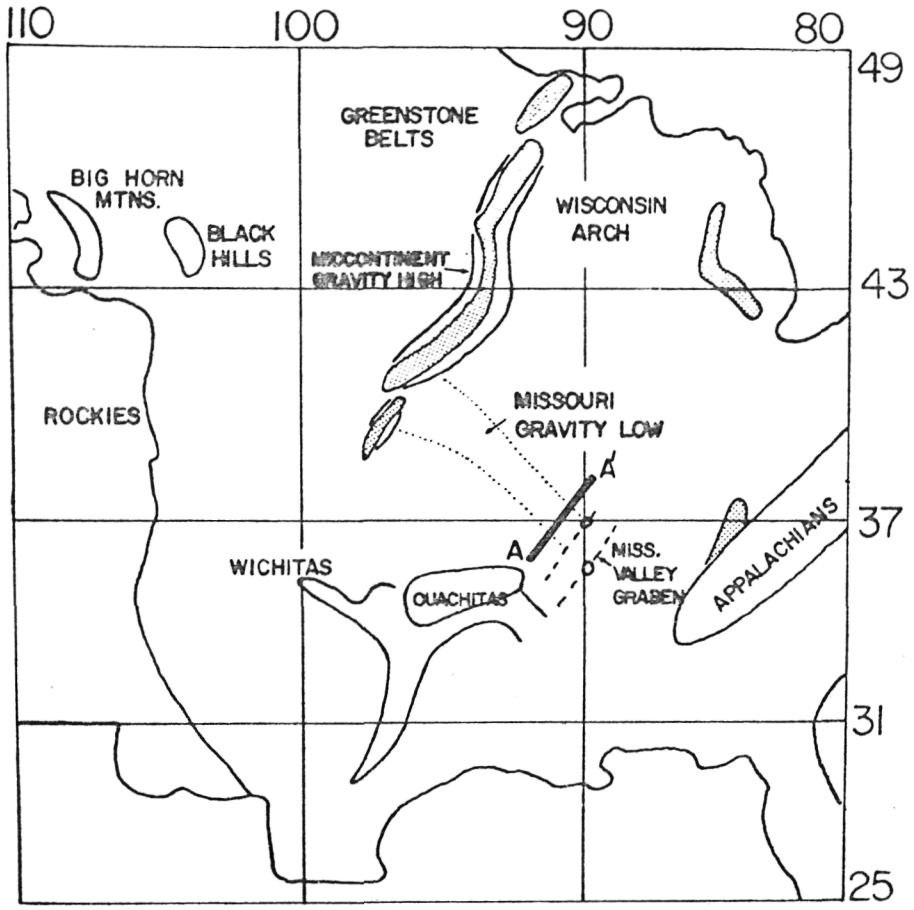

Fig. 4. Sketch map showing major structures delineated in the free air images of Figures 2 and 3 and Plate 1 and equivalent presentations for Bouguer data. The Missouri gravity low is a subtle but pervasive feature that extends from the midcontinent gravity high to the Mississippi embayment. The location of the Mississippi Valley graben is in part from *Kane et al.* [1981]. A-A′ is the location of the profiles shown in Figure 5.

topography, free air, and Bouguer anomalies for this profile are shown in Figure 5. The gravity low exhibits a Bouguer anomaly of −34 mGal for the region beneath the profile. A simple model for the anomaly would be a thickened section of relatively low density sedimentary rock overlying a downwarped region of the Precambrian basement. However, drill holes covering the general area of the Profile A-A′ indicate a typical cover of Paleozoic sediments of only hundreds of meters over the low, with no discernable thinning on either side [*Kisvarsanyi*, 1974]. Thus the gravity signature must be related to an inhomogeneity within the Precambrian basement rocks. *Cordell* [1979] reached a similar conclusion for that part of the low located in the southwestern part of the Rolla quadrangle (37°–38°N latitude, 90°–92°W longitude), where there is a slight local thickening of sedimentary cover over the gravity low.

Some seismic data exist for Missouri that provide information on the possible subsurface configurations of the crust that would give rise to the observed gravity anomaly patterns. *Stewart* [1968] conducted a reversed seismic refraction survey of about 300 km in length along an east-west line in northern Missouri crossing the gravity low at about 39.8°N latitude. Results indicate that the crust consists of three major layers, with average depths of about 5, 20, and 40 km and a $\frac{3}{4}^\circ$ dip toward the west. *Stewart* [1968] also conducted a reversed profile in southern Missouri that extends across the gravity low at about 50 km to the northwest of the gravity profile A-A′ (Figure 4). The refraction data for Stewart's southern profile exhibit very low signal/noise ratios, perhaps because of significant lateral inhomogeneities within the crust. Results are compromised by the low quality of the data, although an argument can be made for a thickened crustal section in the southwestern half of the profile and somewhat higher crustal velocities beneath the northeastern half of the traverse [*Nuttli*, 1976]. Finally, *McCamy and Meyer* [1966] conducted a seismic refraction survey just to the southeast of profile A-A′, reversing a survey done several years earlier. The refraction profile cut across the Bloomfield gravity anomaly and ran in a NE-SW direction within the Mississippi embayment. As discussed by *Ervin and McGinnis* [1975], this region is unusual in that the crust is slightly thicker and underlain by an anomalously high velocity layer as compared to *Stewart*'s [1968] profile in northern Missouri. The anomalous layer probably corresponds to high-density material at the base of the crust, material that may have been emplaced in association with the Precambrian rifting that produced the Reelfoot rift.

In summary, the seismic data suggest a slightly thicker crustal section under the Missouri gravity low, although this interpretation is compromised by poor data and the complicating influence of rocks associated with processes that probably led to formation of the Mississippi embayment. If it

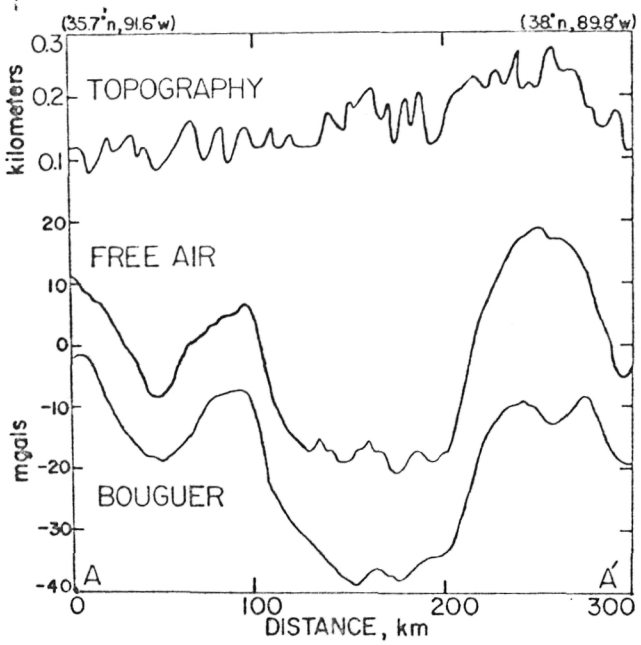

Fig. 5. Topography, free air, and Bouguer anomalies for profile A-A' of Figure 4. The profile cuts across the Missouri gravity low.

is assumed that the Missouri gravity low is due to a thickened crust, then a −34 mGal anomaly, and a density contrast of 0.3 g/cm^3 between crust and mantle, is consistent with a crustal excess of about 3.3 km under the anomaly [*Strebeck*, 1982]. Alternatively, if it is assumed that lateral density variations within the crust cause the gravity anomaly, then the anomaly would be consistent with rocks that were 0.1 g/cm^3 less dense than surrounding materials for the first 4–8 km below the surface [*Strebeck*, 1982]. Of course, other models of crustal inhomogeneities can be generated. However, in the absence of additional seismic or rock type constraints on the crustal structure, they are not worth pursuing at this point.

Relationship of Missouri Gravity Low to Precambrian Rock Provinces and to Magnetic Anomalies

Information on the distribution of Precambrian rock types in Missouri is limited because of the relatively few drill holes that have penetrated into the basement and because of the complexity of the Precambrian geology in the area [*Kisvarsanyi*, 1974; *Bickford et al.*, 1981; *VanSchmus and Bickford*, 1981]. There is, however, a major boundary between 1.61- to 1.65-b.y.-old rocks composed largely of sheared granites and metasediments and younger, 1.38- to 1.48-b.y.-old granites and rhyolites. The boundary runs in a NE-SW direction, as is shown in Plate 2, where the basement rock map of *Bickford et al.* [1981] has been overlain onto a shaded relief map depicting Bouguer anomalies. The Missouri gravity low cuts across the boundary at nearly right angles. On the basis of the rock type data there also appears to be an extension of what are thought to be older metasedimentary rocks into the younger terrain along the gravity low. *Kisvarsanyi* [1974] notes that the area containing the reentrant of older rocks is also a structural high on contour maps depicting the paleotopography of the Precambrian surface and on structural contour maps of Paleozoic sedimentary formations. Presumably, older Precambrian rocks are exposed along the low because of isostatic readjustment and erosion of the younger granites and rhyolites preferentially along the feature.

The observation that the gravity low cuts across the major Precambrian age and rock type boundary in Missouri suggests that the low is related to a structural feature. Further support for this suggestion can be found in the locations of areas with discrete, positive magnetic anomalies. Figure 6 shows regions with vertical intensity magnetic anomalies higher than 600 gammas as black splotches superimposed on the gray tone and shaded relief versions of Bouguer anomalies for Missouri. The 600-gamma contour interval was chosen on the basis of delineating discrete magnetic highs. The magnetic highs are in part clustered along the flanks of the gravity low, i.e., where the gravity gradient is high. Some of the magnetic highs coincide with discrete gravity highs, such as in the area underlain by the Bloomfield intrusion in southeastern Missouri (Figure 6). Clearly, more work needs to be done to establish the pattern of magnetic anomalies in more detail, along with establishing the relationship of the anomaly patterns and the gravity low.

Previous work shows that magnetic highs in Missouri can be correlated with enrichment of magnetite in felsic volcanic rocks and with the presence of mafic and therefore magnetite-rich intrusions [*Allingham*, 1964; *Phelan*, 1969; *Cordell*, 1979]. In addition, local relief with the basement rocks also contributes to low-amplitude anomalies [*Allingham*, 1964]. The location of some of the discrete magnetic highs along the flanks of the gravity low suggests that the flanks correspond to zones of weakness where magmas have intruded. *Kane et al.* [1981] note a similar correlation of magnetic highs along the perimeter of the Mississippi Valley graben. The gravity and magnetic anomaly patterns, and the observation that the gravity low cuts across rock and age provinces, provide strong evidence that the Missouri gravity low is a consequence of a major inhomogeneity within the crust.

Relationships Between Folds, Faults, and Linears in Southern Missouri and Basement Structure

In this section we describe relationships between the Missouri gravity low and the patterns of faults, folds, and linears that exist within the Paleozoic sedimentary rocks covering Missouri. The particular tack that we take is to map the patterns of linear features from HCMM thermal images, compare those linears to the distribution of known faults and folds, and finally relate the trends for the structural data to the gravity low.

Figure 7 shows a HCMM thermal infrared image over southern Missouri taken during relatively clear atmospheric conditions at approximately 1330 LT on June 10, 1978. The frame has been contrast-enhanced and transformed to a Mercator projection. Water appears dark (cool) because it does not warm as quickly as vegetation, soil, or rock. A correlation plot between the apparent temperature seen in this image and the magnitude of topographic slopes demonstrates that the dominant control on temperature is relief. Areas with high relief are relatively dark (cool), while relatively flat regions are bright (warm). For instance, the bright polygonal zone centered at 37.6°N latitude, 90.5°W longitude corresponds to flat terrain underlain in part by igneous rocks of the St. Francois Mountains and in part by the surrounding Cambrian sedimentary rocks. The dark area

Fig. 6. Vertical intensity magnetic anomalies with amplitudes greater than 600 gammas shown as black splotches on gray tone and shaded relief images of Bouguer anomalies for Missouri. Patterns of small black splotches near the southeastern edge of the state and in the upper right are spurious and are remnants from the original digitization of the Missouri magnetic anomaly gap. The arrow points to the Bloomfield magnetic high [*Phelan*, 1969; *Kane et al.*, 1981]. The Bloomfield feature is probably due to a relatively mafic intrusion. Note that many of the magnetic highs are clustered on the edges of the Missouri gravity low. The sun is from the west at 15° above the horizon for the shaded relief data.

to the southwest of this region corresponds to Ordovician carbonates that have been dissected by streams. Flood plains of the streams and the major rivers are flat and therefore relatively bright (hot). Finally, the relatively smooth, bright regions to the north of the Missouri River and east of the Mississippi River coincide with the glacial till deposits related to the Wisconsin and earlier periods of glaciation.

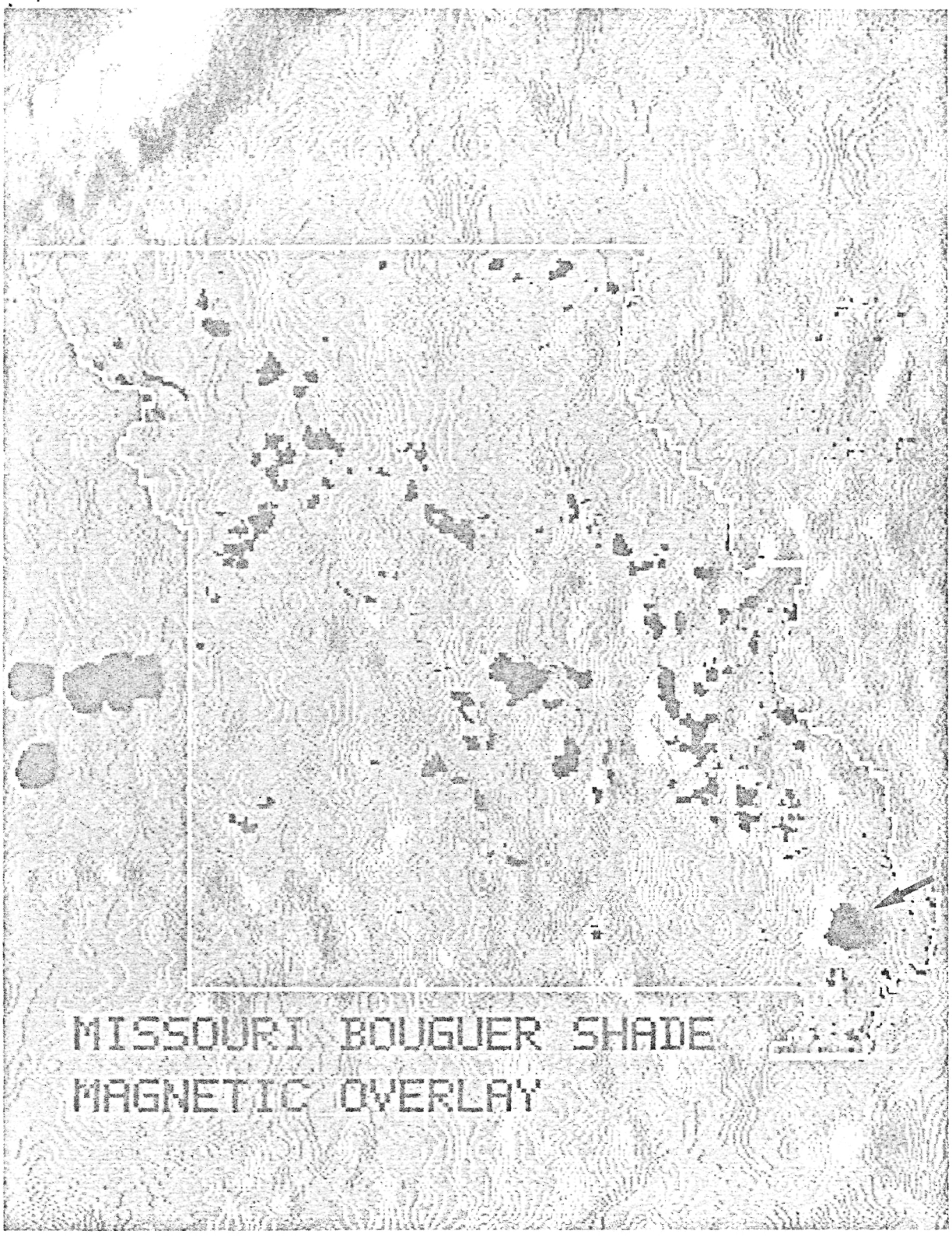

Fig. 6. (continued)

We also combined a shaded relief image of topography with the daytime thermal image by multiplying the two data sets on a element by element basis. The shaded relief map is shown in Figure 8 and the overlay of the IR data onto the relief map is shown in Figure 9. Clearly, linear features are enhanced in the merged data relative to either the shaded relief map or the thermal images shown alone. The reasons are at least threefold. First, topographic linears can be readily discerned on shaded relief maps [*Wise*, 1976]. Second, topographic linears associated with river valleys would be enhanced because of the higher temperatures for the valleys as opposed to the hills. Combining the thermal image

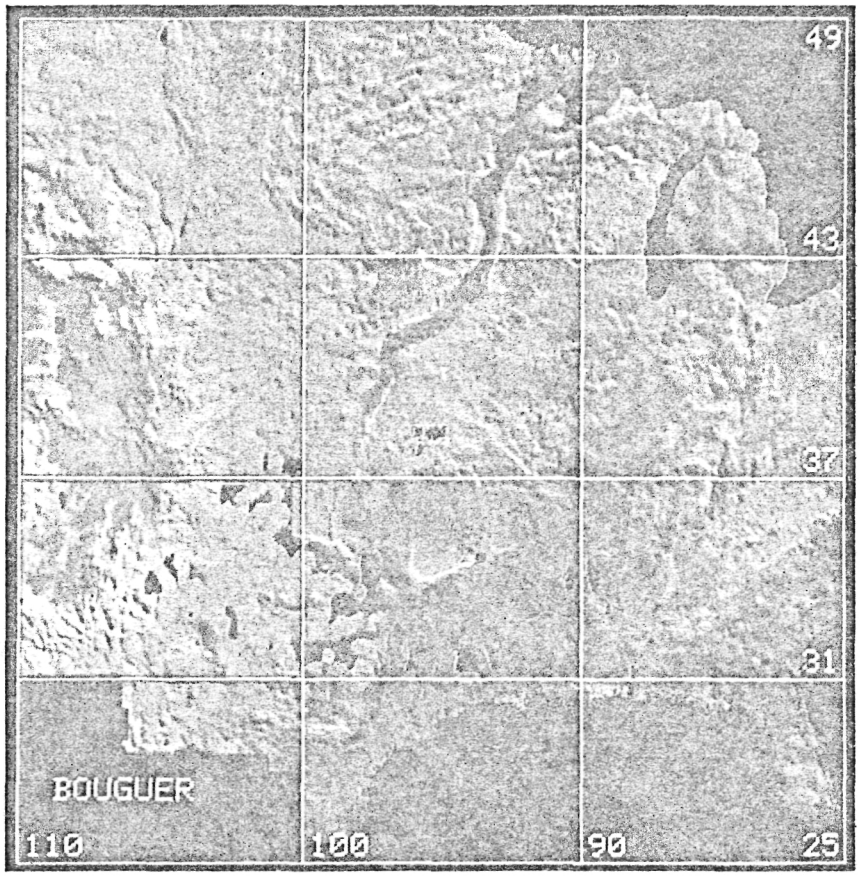

Plate 1. Combination of a color-coded version of the Bouguer image with a shaded relief version of the same data. The effect is to be able to discern both the value of an anomaly for a given region and an indication of the local anomaly gradient. Red corresponds to anomaly values greater than −27 mGal, yellow to orange indicates a range from −74 to −27 mGal, green corresponds to −140 to −27 mGal, blue-green denotes −200 to −140 mGal, and blue corresponds to values smaller than −200 mGal.

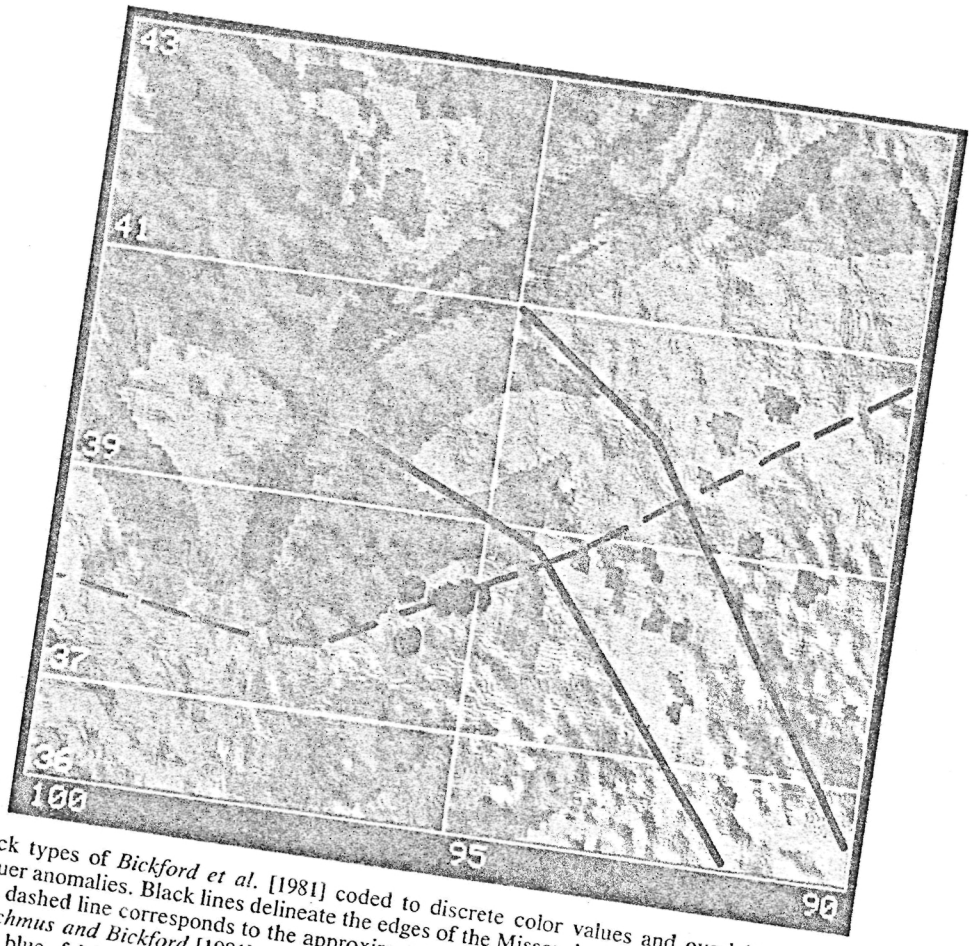

Plate 2. Rock types of *Bickford et al.* [1981] coded to discrete color values and overlaid onto a shaded relief version of Bouguer anomalies. Black lines delineate the edges of the Missouri gravity low as mapped in Figures 2 and 3 and Plate 1. The dashed line corresponds to the approximate boundary between older and younger basement rocks as shown by *VanSchmus and Bickford* [1981]. The sun is from the west at 15° above the horizon. Color values are as follows: medium blue, felsic rocks, mainly sheared granites; yellow, granite; orange, rhyolite; purple, gabbro; dark blue, basalt; red, metasedimentary rocks; green, Sioux quartzite; and light blue, Keweenawan sedimentary rocks. Note that metasedimentary rocks exist to the southeast of the major rock type boundary (between older sheared granites and metasediments and younger granites and rhyolites) along the gravity low.

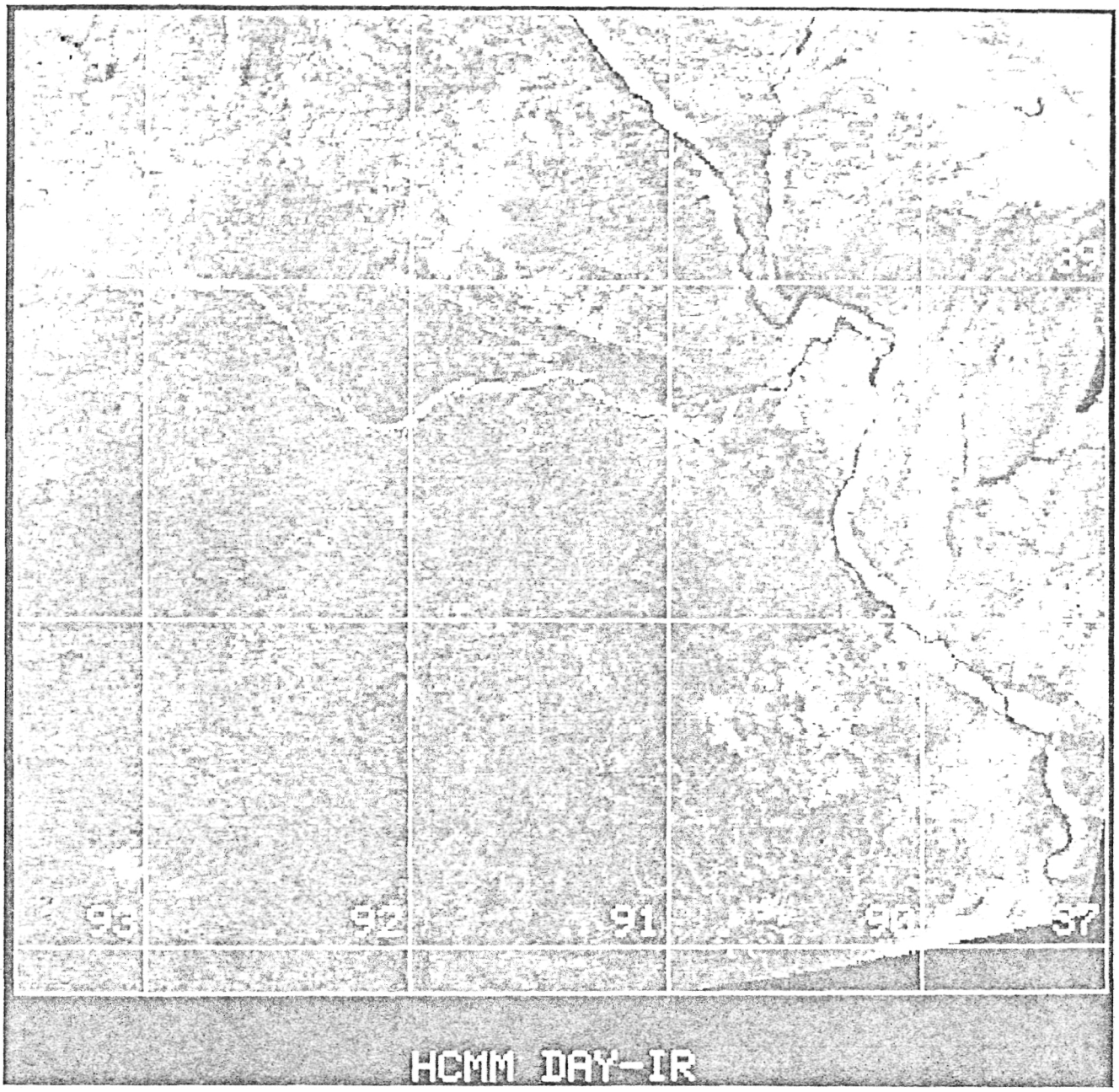

Fig. 7. HCMM daytime thermal infrared image covering southern Missouri that has been contrast-enhanced and transformed to a Mercator projection. Flat areas are brighter (warmer) than regions with high relief. HCMM frame ID A-A0045-19420-2.

with the shaded relief map provides, in effect, a nonlinear enhancement of the topography. Third, any linear thermal features not related to topography would remain in the data. These products were used as our primary base for constructing a linears map for southern Missouri. An apparent thermal inertia image was also constructed using the formulation of *Price* [1977] and overlaid onto the shaded relief image. However, this product did not provide a significant amount of additional information, probably because the nighttime thermal and the albedo data contain only 25% of 13% of the variance inherent in the three-dimensional thermal day–thermal night–albedo data set.

Figure 10 is a sketch map showing linears from the processed HCMM data. Also shown are folds from the Missouri structural map [*McCracken*, 1971] and faults from the latest geologic map of the state [*Anderson*, 1979]. The folds are thought to be drape folds over the Precambrian surface in areas with significant relief due to basement faulting [*McCracken*, 1971]. Most of the faults are high-angle normal faults, although some evidence for shear movement can be found [*McCracken*, 1971]. The area occupied by the high-temperature region of the St. Francois Mountains and surroundings is also drawn in Figure 10. Note that linears, faults, and folds generally strike in a direction parallel to the gravity low. Also, the sharp southwestern edge of the St. Francois Mountains is coincident with the northern flank of the low. Further away from the low the azimuths of features tend to disperse. Clearly, the basement inhomogeneity associated with the Missouri gravity low has had a pronounced influence on the pattern of faulting and folding that has

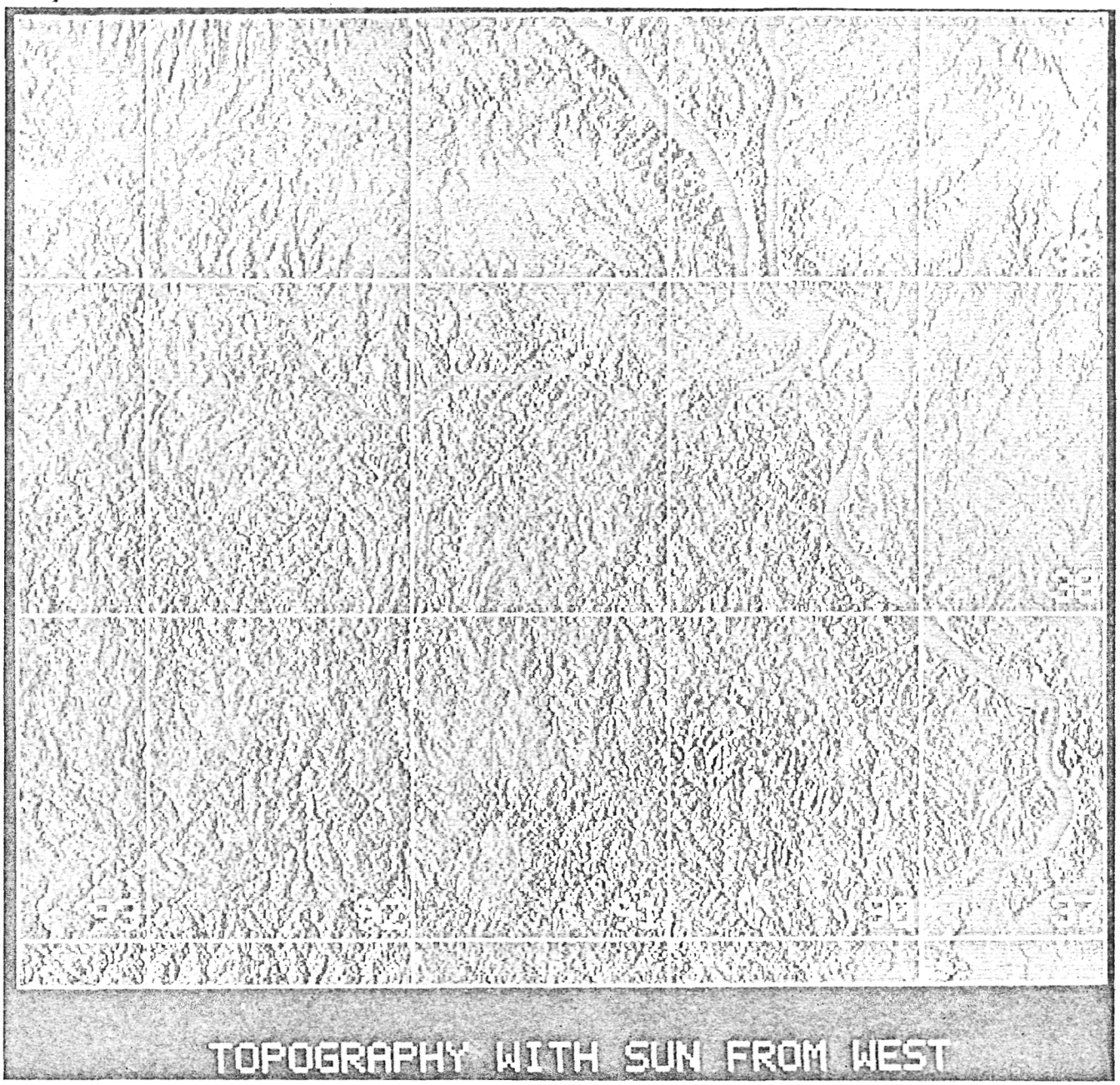

Fig. 8. Shaded relief map depicting topography for southern Missouri and western Illinois, with the sun at 20° above the western horizon.

propagated through the Paleozoic sedimentary cover. The preponderance of normal faulting in the area implies, as does the reentrant of older basement rocks along the gravity low, that the dominant structural activity associated with the crustal inhomogeneity beneath the gravity low has been one of vertical readjustment. Preferential uplift along the low is also consistent with the pattern of vertical displacements shown by the mapped faults in the area (Figure 10).

THE AGE, ORIGIN, AND EVOLUTION OF THE MISSOURI GRAVITY LOW

The Missouri gravity low must be older than the Paleozoic sediments that have been deposited over the reentrant of older rocks into the granite-rhyolite terrain. The reason is that any uplift and stripping of the younger granite-rhyolite rocks along the gravity low must have occurred before the Precambrian surface was buried. The oldest abundant sedimentary rocks in southern Missouri consist of Upper Cambrian sandstones called the Lamotte Formation [*Anderson*, 1979].

A number of events affected the region now occupied by the gravity low during the Precambrian, including (1) the set of processes that led to formation of the granite-rhyolite terrain of southern Missouri (*Bickford et al.* [1981] speculate that a rifting event or a convergent plate margin might explain formation of the granite-rhyolite units), (2) rifting that was associated with the opening of the Reelfoot basin, the Precambrian precursor to the Mississippi embayment [*Ervin and McGinnis*, 1975], (3) rifting associated with formation of the midcontinent gravity high [*Chase and*

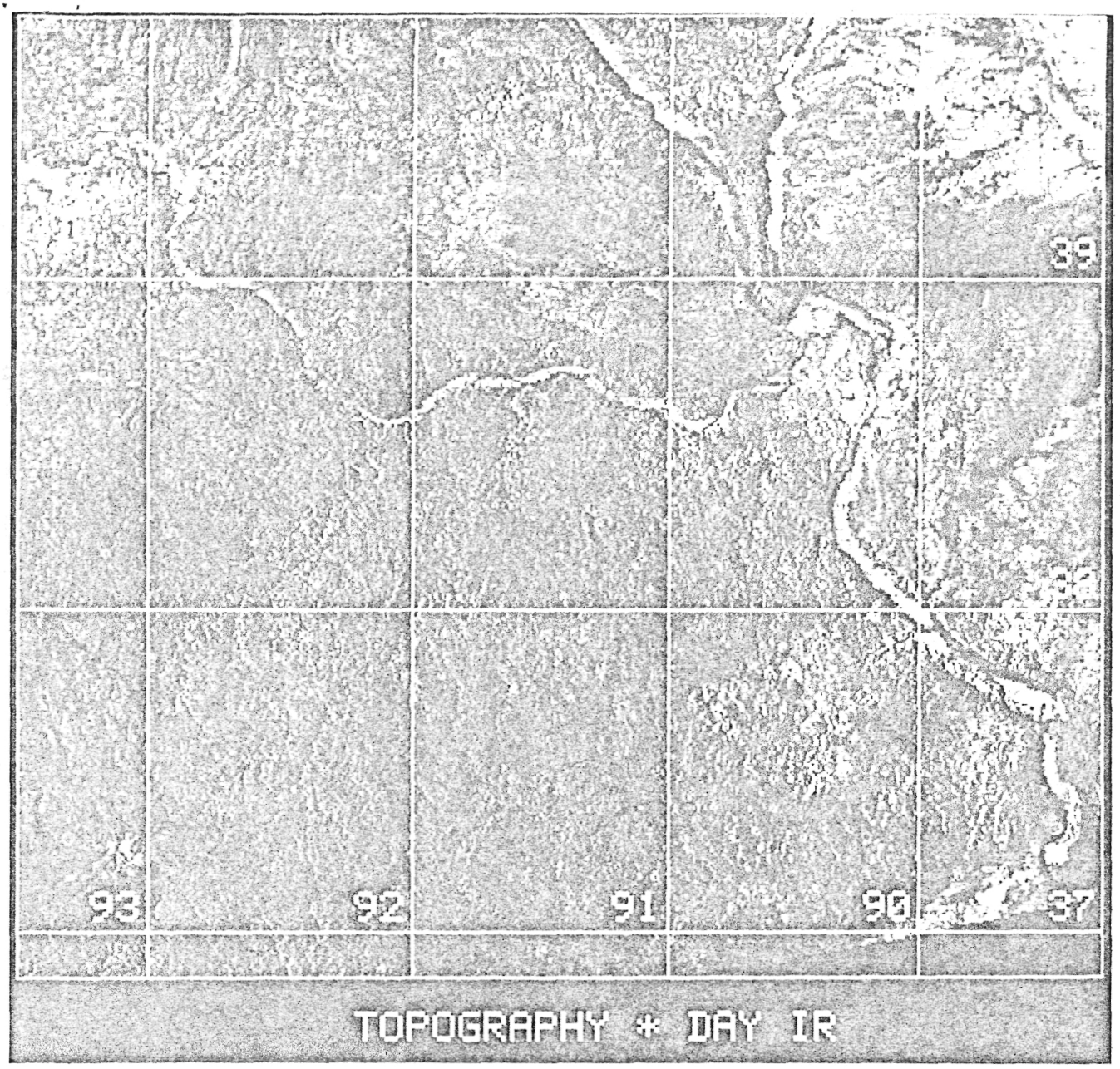

Fig. 9. HCMM contrast-enhanced daytime thermal infrared image overlaid onto a shaded relief image depicting topography. The sun for the shaded relief image is from the west at 20° above the horizon. The overlay tends to enhance subtle topographic features while retaining linear thermal anomalies not associated with relief.

Gilmer, 1973], and (4) the postulated continent-continent collision associated with the Grenville orogeny [*Dewey and Burke*, 1973].

At this point it is useful to summarize the characteristics of the Missouri gravity low. The feature has a Bouguer amplitude anomaly of about −34 mGal in southeastern Missouri, has a width varying from 120 to 160 km, and extends about 700 km in length. The flanks of the feature are the locations of some of the magnetic highs in Missouri. Finally, the feature controls the pattern of normal faulting in the Precambrian basement rocks and overlying sedimentary cover. Except for the lack of a discernible thickness of sedimentary fill overlying the granite-rhyolite terrain, such a description is consistent with description of a failed arm of a triple junction [*Burke and Whiteman*, 1973]. There are examples of relatively recent rifts that have negative anomalies with no associated sediment fill, although *Burke and Whiteman* [1973] interpret these anomalies as being due to ponding of magmas at the base of the crust.

The Missouri gravity low could have formed as the failed arm of a triple junction that existed before formation of the granite-rhyolite terrain. The triple junction site would have been to the southeast, with the other two rifts becoming active spreading centers. Closure of that spreading center, with subsequent continent-continent collision, may have been the most plausible method of generating the abundant alkalic igneous activity that produced the younger granite-rhyolite terrain. In the process, most of the sediment fill within the failed rift would have been metamorphosed, intruded into, and covered by the alkalic magmas associated with formation of the granite-rhyolite terrain. The metasediments found in the reentrant of older rocks in this terrain

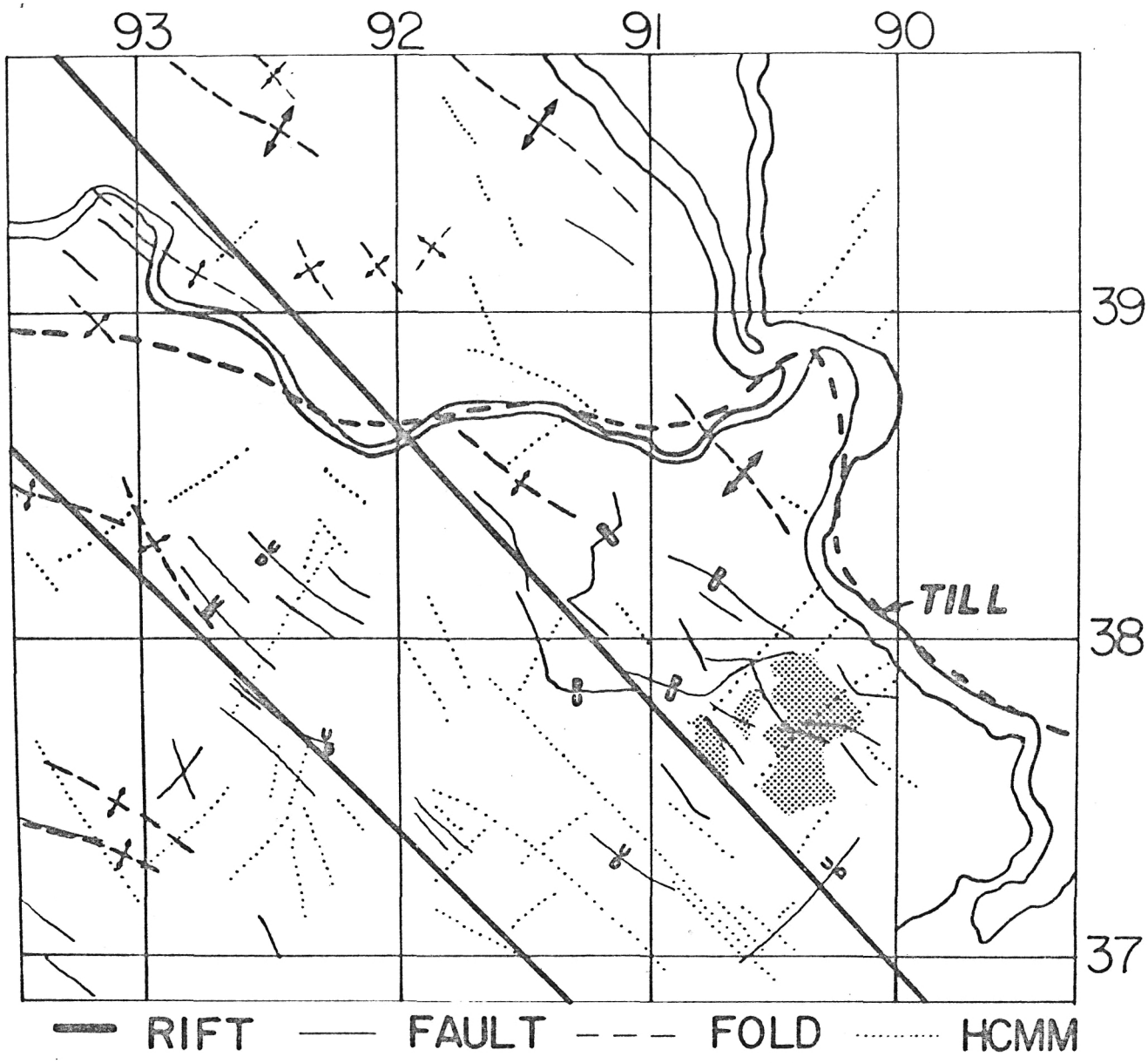

Fig.10. Sketch map showing the Missouri gravity low, mapped faults and folds, and linears as mapped from the HCMM thermal image and from the thermal topography overlay. Heavy solid lines indicate the borders of the Missouri gravity low as seen in the gravity anomaly images. The structural trend is dominated by the trend of the Missouri gravity low. Azimuths of structures tend to disperse for regions far from the low.

(Plate 2) may be the remnants of this valley fill. Subsequent events, such as the formation of the Reelfoot rift, which is postulated to have occurred at approximately 1.1 b.y. [*Ervin and McGinnis,* 1975], or recently proposed triple-pronged northern extensions of the Reelfoot [*Braile et al.,* 1982], could have served to reactivate parts of the rift. Reactivation certainly occurred during the mid-Paleozoic to Mesozoic, when the southeastern end of the low was structurally active as the Pascola arch. Reactivation events may be the cause of the variable characteristics of the feature along its length. We stress that our interpretation, although plausible, is by no means unique and serves only as a working hypothesis to be updated or discarded as new seismic, potential field, and rock type data are acquired. It is of interest to note that an origin as a failed rift arm may provide a new perspective on the source of the Pb-Zn-Cu in the Paleozoic sedimentary cover, since base metal mineralization is a common process associated with rifting events.

SUMMARY AND IMPLICATIONS

1. Standard digital image-processing techniques have been used to interpolate and display free air and Bouguer anomalies and topography as gray tone, color-coded, and shaded relief images as part of an analysis of how structural features within the Precambrian basement of Missouri relate to the broader structure of the midcontinent. In addition, the Precambrian basement rock type map of *Bickford et al.* [1981] and magnetic anomalies for Missouri have been digitally merged and displayed with the gravity data to facilitate examination of correlations. Finally, Heat Capacity Mapping Mission thermal infrared data covering southern

Missouri have been enhanced and overlaid onto shaded relief versions of topography.

2. A major and previously unrecognized gravity anomaly (Missouri graivty low) in the midcontinent is 700 km long, 120–160 km wide, and exhibits a Bouguer amplitude of −34 mGal in southeastern Missouri. The low begins at a break in the midcontinent gravity high in southeastern Nebraska, extends in a southeast direction through Missouri, and intersects the Mississippi Valley graben as defined by *Kane et al.* [1981]. The northern and southern edges of the intersection of the Missouri gravity low and the Mississippi Valley graben are the sites of discrete positive gravity anomalies that are thought to be due to plutons. Also, many of the epicenters associated with the New Madrid seismic area are within the crustal block defined by the intersection of the gravity low and the Mississippi Valley graben. Some discrete positive magnetic anomalies exist along the flanks of the Missouri gravity low. Finally, the gravity low may be the site of a reentrant of older Precambrian metasedimentary rocks into the younger granites and rhyolites that underlie much of southern Missouri. The amplitude of the low is too high to be related to thickening of Paleozoic sedimentary rocks. Rather, the anomaly is probably due to a basement inhomogeneity. Two seismic refraction profiles [*Stewart*, 1968] cut across the low in Missouri. In both cases the seismic data are consistent with a slightly thicker crustal section beneath the gravity low. The magnitude of the gravity anomaly is consistent with a crustal excess of 3.3 km as compared to surrounding areas or with a crust that is slightly less dense (0.1 g/cm^3 contrast) in the upper 4–8 km.

3. A HCMM daytime thermal image was overlaid onto a shaded relief image of topography covering the area underlain by the gravity low in southern Missouri. These data show that linears trend in the same direction as the low. Mapped faults (mainly high-angle normal faults) and drape folds over basement relief in the Paleozoic sedimentary cover of southern Missouri follow a similar pattern. Some of the HCMM linears correspond to the mapped structures, in some cases they are extensions of such features, and some linears do not correspond to mapped features. In any case, the correlation of the gravity low and the structural data suggest that the low is a major basement rift and that the structures in the Paleozoic deposits are due to vertical readjustments related to the crustal inhomogeneity that gives rise to the low.

4. The Missouri gravity low is older than the oldest Paleozoic sedimentary rocks that cover the reentrant of metasedimentary rocks into the younger granites and rhyolites. The oldest rocks correspond to the Upper Cambrian Lamotte Formation. The gravity low could be the present expression of a failed arm of a triple junction that existed before or during the events that led to the younger granite-rhyolite terrain of southern Missouri. Emplacement of the igneous rocks would have effectively covered or metamorphosed sedimentary rocks that formed as valley fill within the rift. Reactivation of the rift has certainly taken place since it formed. Association of the Missouri gravity low with a unique history is difficult at this point because of lack of information on basement rock types, ages, and seismic controls on crustal configurations beneath the low.

Acknowledgments. This work was carried out with funding from the NASA Office of Space and Terrestrial Applications, Non-Renewable Earth Resources, through a contract (955959) from the Jet Propulsion Laboratory and by the Heat Capacity Mapping Mission Data Analysis Program, Goddard Space Flight Center, under contract NAS5-26533. Processing was conducted with a PDP-11/34 system located within the Washington University Regional Planetary Image Facility. Thanks are extended to St. Louis University for seismic data and to the Geopositional Division, Defense Mapping Aerospace Agency Center, St. Louis, Missouri, for gravity data. Thanks must go to L. Miller for providing much help in preparing this manuscript. Conversations with M. E. Bickford, E. Kisvarsanyi, and O. Nuttli and reviews by M. Londe, R. Batiza, M. Settle, and two anonymous scientists have played an important role in allowing us to integrate the information discussed in this paper.

REFERENCES

Allingham, J. W., Low-amplitude aeromagnetic anomalies in southeastern Missouri, *Geophysics, 4*, 537–552, 1964.

Anderson, K. H., Geologic Map of Missouri, Mo. Geol. Surv., Rolla, 1979.

Arvidson, R. E., E. A. Guinness, J. Strebeck, G. Davies, and K. J. Schulz, Image processing applied to gravity and topography data covering the continental United States, *Eos Trans. AGU, 63*, 261–265, 1982.

Batson, R. M., K. Edwards, and E. M. Eliason, Computer-generated shaded relief images, *J. Res. U.S. Geol. Surv., 3*, 401–408, 1975.

Bickford, M. E., K. L. Harrower, W. J. Hoppe, B. K. Nelson, R. L. Nusbaum, and J. J. Thomas, Rb-Sr and U-Pb geochronology and distribution of rock types in the Precambrian basement of Missouri and Kansas, *Geol. Soc. Am. Bull., 92*, 323–341, 1981.

Braile, L. W., G. R. Keller, W. J. Hinze, and E. G. Lidiak, An ancient rift complex and its relationship to contemporary seismicity in the New Madrid seismic zone, *Tectonics, 1*, 225–237, 1982.

Burke, K., and A. J. Whiteman, Uplift, rifting, and break-up of Africa, in *Implications of Continental Drift to the Earth Sciences*, edited by D. H. Tarling and S. K. Runcorn, pp. 735–755, Academic, New York, 1973.

Chase, C. G., and T. H. Gilmer, Precambrian plate tectonics: The midcontinent gravity high, *Earth Planet. Sci. Lett., 21*, 70–78, 1973.

Cordell, L., Gravity and aeromagnetic anomalies over basement structure in the Rolla quadrangle and the S.E. Missouri lead district, *Econ. Geol., 67*, 409–425, 1979.

Dewey, J. F., and K. Burke, Tibetan, Variscan, and Precambrian basement reactivation: Products of continental collision, *J. Geol., 81*, 683–692, 1973.

Eliason, E., and L. A. Soderblom, An array processing system for lunar geochemical and geophysical data, *Proc. Lunar Planet. Sci. Conf. 8th*, 1163–1170, 1977.

Ervin, C. P., and L. D. McGinnis, Reelfoot rift: Reactivated precursor to the Mississippi embayment, *Geol. Soc. Am. Bull., 86*, 1287–1295, 1975.

Evans, L. L., Geology of the Brushy Creek Mine, Viburnum Trend, southeast Missouri, *Econ. Geol., 72*, 381–390, 1977.

Gerdemann, P. E., and H. E. Meyers, Relationships of carbonate facies patterns to ore distribution and to ore genesis in the S. E. Missouri lead district, *Econ. Geol., 67*, 426–433, 1972.

Grundmann, W. H., Geology of the Viburnum No. 27 Mine, Viburnum Trend, southeast Missouri, *Econ. Geol., 72*, 349–364, 1977.

Kahle, A. B., and A. R. Gillespie, and A. F. H. Goetz, Thermal inertia imaging—A new geologic mapping tool, *Geophys. Res. Lett., 3*, 26–28, 1976.

Kane, M. F., T. G. Hildenbrand, and J. D. Hendricks, Model for the tectonic evolution of the Mississippi embayment and its contemporary seismicity, *Geology, 9*, 563–568, 1981.

Kisvarsanyi, E. B., Operation basement: Buried Precambrian rocks of Missouri—Their petrography and structure, *Am. Assoc. Pet. Geol. Bull., 58*, 674–684, 1974.

Kisvarsanyi, G., Precambrian metallogenesis in the St. Francois Mtns. igneous province, S. E. Missouri, Studies in Precambrian Geology of Missouri, *Rep. Invest. Mo. Geol. Surv., 61*, 164–173, 1976.

Kisvarsanyi, G., and E. B. Kisvarsanyi, Ortho-polygonal tectonic patterns in the exposed and buried Precambrian basement of southeast Missouri, Proceedings of the First International Conference on the New Basement Tectonics, *Utah Geol. Assoc. Publ., 5*, 169–182, 1976.

Kobrick, M., Topography of the terrestrial planets, *Astronomy, 10,* 18–22, 1982.

McCamy, K., and R. P. Meyer, Crustal results of fixed multiple shots in the Mississippi embayment, in *The Earth Beneath the Continents, Geophys. Monogr. Ser.,* vol. 10, edited by J. S. Steinhart and T. J. Smith, pp. 370–381, AGU, Washington, D. C., 1966.

McCracken, M. H., Structural features of Missouri, *Rep. Invest. Mo. Geol. Surv., 44,* 68 pp., 1971.

McGinnis, L. D., M. G. Wolf, J. J. Kohsmann, and C. P. Ervin, Regional free air anomalies and tectonic observations in the United States, *J. Geophys. Res., 84,* 591–601, 1979.

Moik, J. G., Digital processing of remotely sensed images, *NASA Spec. Publ. SP-431,* 330 pp., 1980.

Mouat, M. M., and C. W. Clendenin, Geology of the Ozark Lead Company Mine, Viburnum Trend, southeast Missouri, *Econ. Geol., 72,* 398–407, 1977.

Nuttli, O. W., Seismological studies of Missouri crustal structure, Studies in Precambrian Geology of Missouri, *Rep. Invest. Mo. Geol. Surv., 61,* 184–189, 1976.

Offield, T. W., Thermal infrared images as a basis for structure mapping, Front range and adjacent plains in Colorado, *Geol. Soc. Am. Bull., 86,* 495–502, 1975.

Paarlberg, N. L., and L. L. Evans, Geology of the Fletcher Mine, Viburnum Trend, southeast Missouri, *Econ. Geol., 72,* 391–397, 1977.

Pettengill, G., E. Eliason, P. Ford, G. Loriot, and H. Masursky, Pioneer Venus radar results: Altimetry and surface processes, *J. Geophys. Res., 85,* 8261–8270, 1980.

Phelan, M. J., Crustal structure in the central Mississippi Valley earthquake zone, Ph.D dissertation, Washington Univ., St. Louis, Mo., 1969.

Price, J. C., Thermal inertia mapping: A new view of the earth, *J. Geophys. Res., 82,* 2582–2590, 1977.

Russ, D. P., The structure of the Reelfoot rift and its relationship to some regional midcontinent features, *Geol. Soc. Am., Abstr. Programs, 13,* 543, 1981.

Sabins, F. F., Thermal infrared imagery and its application to structural mapping in southern California, *Geol Soc. Am. Bull., 80,* 397–404, 1969.

Simpson, R. W., and R. H. Godson, Colored gravity anomaly and terrain maps of the east central United States, *U.S. Geol. Surv. Open File Rep. 81-846,* 1981.

Stauder, W., M. Kramer, G. Fischer, S. Schaeffer, and S. T. Morrissey, Seismic characteristics of southeast Missouri as indicated by a regional telemetered microearthquake array, *Bull. Seismol. Soc. Am., 66,* 1953–1964, 1977.

Stewart, S. W., Crustal structure in Missouri by seismic refraction methods, *Bull. Seismol. Soc. Am., 58,* 291–323, 1968.

Strebeck, J. W., Structure of the Precambrian basement in the Ozark plateau as inferred from gravity and remote sensing data, M. S. thesis, Washington Univ., St. Louis, Mo., 1982.

Sweeney, P. H., E. D. Harrison, and M. Bradley, Geology of the Magmont Mine, Viburnum Trend, southeast Missouri, *Econ. Geol., 72,* 365–371, 1977.

VanSchmus, W. R., and M. E. Bickford, Proterozoic chronology and evolution of the midcontinent region, North America, in *Precambrian Plate Tectonics,* edited by A. Kromer, pp. 261–296, Elsevier, New York, 1981.

Watson, K., Geologic applications of thermal inertia mapping from HCMM, paper presented at International Geoscience and Remote Sensing Symposium, Inst. of Electr. and Electron. Eng., New York, 1981.

Wise, D. U., Sub-continental size fracture systems etched into the topography of New England, Proceedings of the First International Conference on the New Basement Tectonics, *Utah Geol. Assoc. Publ., 5,* 416–422, 1976.

Woollard, G. P., and H. R. Joesting, Bouguer gravity anomaly map of the United States, U.S. Geol. Surv., Reston, Va., 1964.

(Received November 16, 1981;
revised June 10, 1982;
accepted July 13, 1982.)

APPENDIX TWO

TRANSFORMATION FROM RED, GREEN, AND BLUE (RGB) TO HUE, SATURATION, AND INTENSITY (HSI)

It is often useful to consider the brightness values of an image triplet (i.e., three images taken at different times or different wavelengths over the same area) as points in a three-dimensional coordinate system. The coordinate axes can be defined such that each point is represented by parameters used to describe color. For instance, the three axes can represent intensities of the three primary colors blue, green, and red. This RGB space is limited by the dynamic range available to an image. For example, each element of a Landsat MSS image in bands 4 to 6 has a range of 0 to 127. Any data point must then fall within a cube defined by the R-G, G-B, and R-B planes and with sides of length equal to 127. The cube lies in the first octant of the RGB coordinate system so that values of R, G, and B are never negative. Another example of an RGB space is shown in Figure 1 where the maximum value is 255 instead of 127.

Another representation of color is the hue, saturation, and intensity (HSI) model. Hue is defined as the dominant wavelength of a color. For example, an equal mixture of red and green results in a hue of yellow. Saturation is a measure of the purity of a color. A completely unsaturated color (gray tone) is an equal mixture of the three primaries (or an equivalent mixture of three or more distinct hues), whereas a fully saturated or pure color can be

created by mixing no more than two of the primaries. The intensity of a color is a measure of how bright a color appears.

Hue, saturation, and intensity can be expressed as spherical coordinates that are related to the RGB coordinates described above. Along the line where R, G, and B are equal lies the gray vector, so-called because points along it correspond to varying shades of gray. This vector direction can also define the x axis for a second set of Cartesian coordinates (Figure 2). Let the positive y axis lie in the B-G plane at a +45 degree angle from the G axis. All coordinates are right-handed so a positive angle denotes counterclockwise rotation. By the definition of a right-handed coordinate system, the positive z axis would be at a 135 degree angle from the positive G axis and inclined 37.26 degrees from the positive R axis. Intensity, hue, and saturation can then be defined as spherical coordinates where:

$$H = \arctan (y/z) \qquad (1)$$

$$S = \arccos x/(x^2 + y^2 + z^2)^{1/2} \qquad (2)$$

$$I = (x^2 + y^2 + z^2)^{1/2} \qquad (3)$$

One can convert RGB to xyz by the following matrix operations:

$$\begin{pmatrix} R \\ G \\ B \end{pmatrix} (Y) \quad (Z) = \begin{pmatrix} x \\ y \\ z \end{pmatrix} \qquad (4)$$

where Z and Y are rotation matrices which describe rotations of 45 degrees about the R axis and of -35.26 degrees about the G axis, respectively. Note again that all coordinates are right-handed and a positive angle of rotation moves the rotated axes counterclockwise

as seen looking down the axis of rotation.

The inverse transform equations are then:

$$x = I \cos(S) \qquad (5)$$
$$y = I \sin(S) \sin(H) \qquad (6)$$
$$z = I \sin(S) \cos(H) \qquad (7)$$

and

$$\begin{pmatrix} x \\ y \\ z \end{pmatrix} (-Z) \quad (-Y) = \begin{pmatrix} R \\ G \\ B \end{pmatrix} \qquad (8)$$

where -Z and -Y are the same rotation matrices as above with the angles negated.

As mentioned above, any color is constrained to lie within the cube shown in Figure 1. Intensity, hue, and saturation values must be normalized so that each not only fills the allowed dynamic range, but also so that points of maximum saturation and intensity lie on the cubic constraining surface. Thus:

$$H' = MAX\ (H/L) \qquad (9)$$
$$S' = MAX\ (S/M) \qquad (10)$$
$$I' = MAX\ (I/N) \qquad (11)$$

where: MAX is the maximum value allowed along the RGB axes (i.e. the dynamic range) and L, M, and N are the respective normalization factors for H, S, and I. The value of L can be derived easily; hue values range from 0 to 360 so L=360. Thus:

$$H' = MAX\ (H/360) \qquad (12)$$

M, however, is a function of hue and N is a function of both

hue and saturation. To find M and N we will first look at the projection of the cube in Figure 1 onto the y-z plane (Figure 3). For the purpose of this derivation the cube is treated as if each side were one unit in length. The x,y,z coordinates of the cube vertices correspond to black and white and to the colors red, green, blue, yellow, cyan, and purple with maximum saturation and intensity. These vertices have the following coordinates:

	x	y	z
Red	$1/(3)^{1/2}$	0	$(2/3)^{1/2}$
Yellow	$2/(3)^{1/2}$	$1/(2)^{1/2}$	$1/(6)^{1/2}$
Green	$1/(3)^{1/2}$	$1/(2)^{1/2}$	$-1/(6)^{1/2}$
Cyan	$2/(3)^{1/2}$	0	$-(2/3)^{1/2}$
Blue	$1/(3)^{1/2}$	$-1/(2)^{1/2}$	$-1/(6)^{1/2}$
Purple	$2/(3)^{1/2}$	$-1/(2)^{1/2}$	$1/(6)^{1/2}$
White	3	0	0
Black	0	0	0

Projecting some point of maximum saturation P onto the y-z plane we find the lengths LEN and OUT using the Law of Sines (Figure 3).

$$OUT = (2)^{1/2}/\sin(120-H) \qquad (13)$$
$$LEN = (2/3)^{1/2}\sin(H)/\sin(120-H) \qquad (14)$$

Next we must find the x coordinate of P. Considering the x,y,z coordinate system of Figure 2, define a triangle by constructing a vertical line between the point Yellow to the y-z plane, a horizontal line from the point Red to this vertical line, and a line

between the points Red and Yellow (Figure 4). The angle between RY and the horizontal can be defined as PSI where:

$$PSI = \arctan(1/2)^{1/2} \qquad (15)$$

Then X, the x coordinate of P, is the x coordinate of Red plus some distance determined by LEN that we shall call UP.

$$UP = LEN \tan(PSI) = LEN/(2)^{1/2} \qquad (16)$$

thus:

$$X = (1/3)^{1/2} + UP \qquad (17)$$

To find maximum saturation define a triangle with vertices at the origin, at P, and at the projection of P onto the gray vector (x axis). Then M, the maximum saturation, has the form:

$$M(H) = \arctan(OUT/X) \qquad (18)$$

To find N, the maximum intensity function, first define an additional triangle with vertices P, White, and the projection of P onto the x axis (Figure 5). The angle between the horizontal and the line from P to White is then THETA, where:

$$THETA = \arctan((3)^{1/2}-X)/OUT \qquad (19)$$

This angle is constant for a given hue (i.e., independent of saturation). To find the maximum intensity construct a triangle defined by the points White, the origin, and a point P' (Figure 6). P' is a point of arbitrary hue and saturation but maximum allowed

intensity. Using the Law of Sines we find:

$$N = (3)^{1/2}\cos(THETA)/\sin(THETA+90-S) \qquad (20)$$

The solution, thus far, is valid only for angles of hue between 0 and 60 degrees. To remedy this problem a function D(H) is used to effectively fold hues into a 0 to 60 degree range and leave our solutions intact. D(H) has the following form:

$$D = \begin{cases} 360-H & H > 300 \\ 240-H & 180 < H < 300 \\ 120-H & 60 < H < 180 \\ H & H < 60 \end{cases} \qquad (21)$$

The derivation remains the same except D replaces H in equations (13) and (14).

Thus L, M, and N have been found and may be used to create image representations of hue, saturation, and intensity. An enhancement of an image using this technique, consists of transforming an RGB image to HSI, contrast enhancing the hue, saturation, and intensity separately so that each fills the available dynamic range, and inverting the transform equations to create an enhanced RGB image. Alternately, 3 images can be assigned to hue, saturation, and intensity, contrast enhanced, transformed to RGB coordinates, and a color image generated.

APPENDIX II - FIGURE CAPTIONS

Figure 1: An RGB space with a dynamic range of 0 to 255 DN. The gray vector consists of all points where R=G=B. Each point inside or on the constraining surface is a unique color.

Figure 2: Geometric model of the HSI representation of color. The x-axis lies along the gray vector of RGB space. Each point in this coordinate system is a unique intensity (vector length), hue (azimuth), and saturation (colatitude). the x, y, and z axes are orthogonal axes used as an intermediate step between RGB and HSI coordinates.

Figure 3: Projection of the cubic constraining surface in Figure 1 onto the y-z plane of the system shown in Figure 2. The hexagon is the outline of a shadow cast by the cube with parallel light shining down the x-axis. H is the anlge of hue. the projections of the cube vertices are labeled according to their hue (i.e., green, yellow, cyan, etc.).

Figure 4: The triangle defined by the line between the points Red and Yellow, a vertical line (i.e., parallel to the x-axis) from the point Yellow to the y-z plane, and a horizontal line (i.e., parallel to the y-z plane) that

intersects the vertical line.

Figure 5: The triangle defined by the points White, Black, P, and the projection of P onto the x-axis. M is the angle of maximum saturation. P is a point of arbitary hue, but maximum saturation and intensity.

Figure 6: The triangle is defined by Black, White, and P'. S is the angle of saturation, N is the maximum intensity for that S and a given hue, and P' is apoint of maximum intensity for the same S and a given hue.

Figure 1

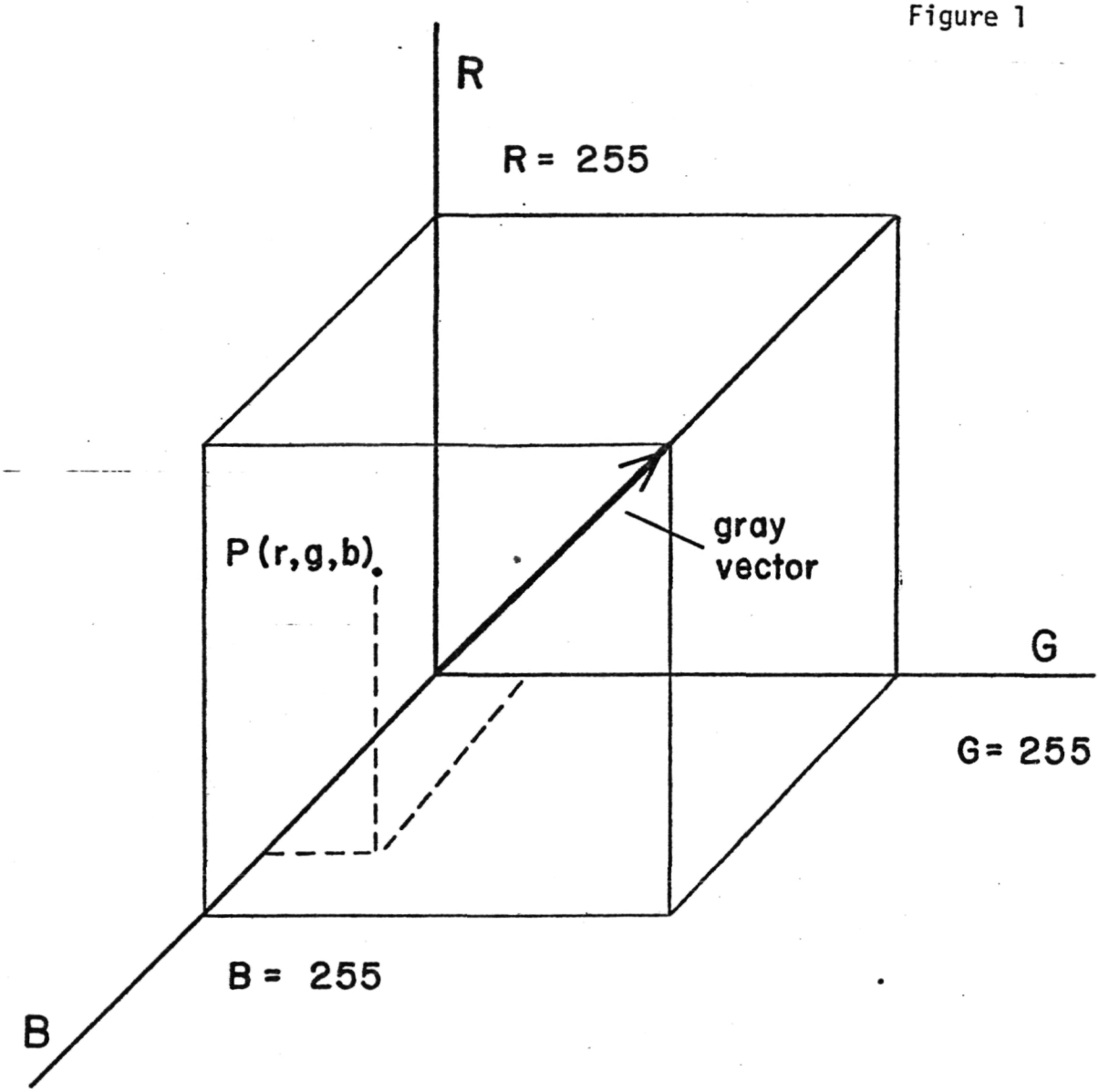

Figure 2

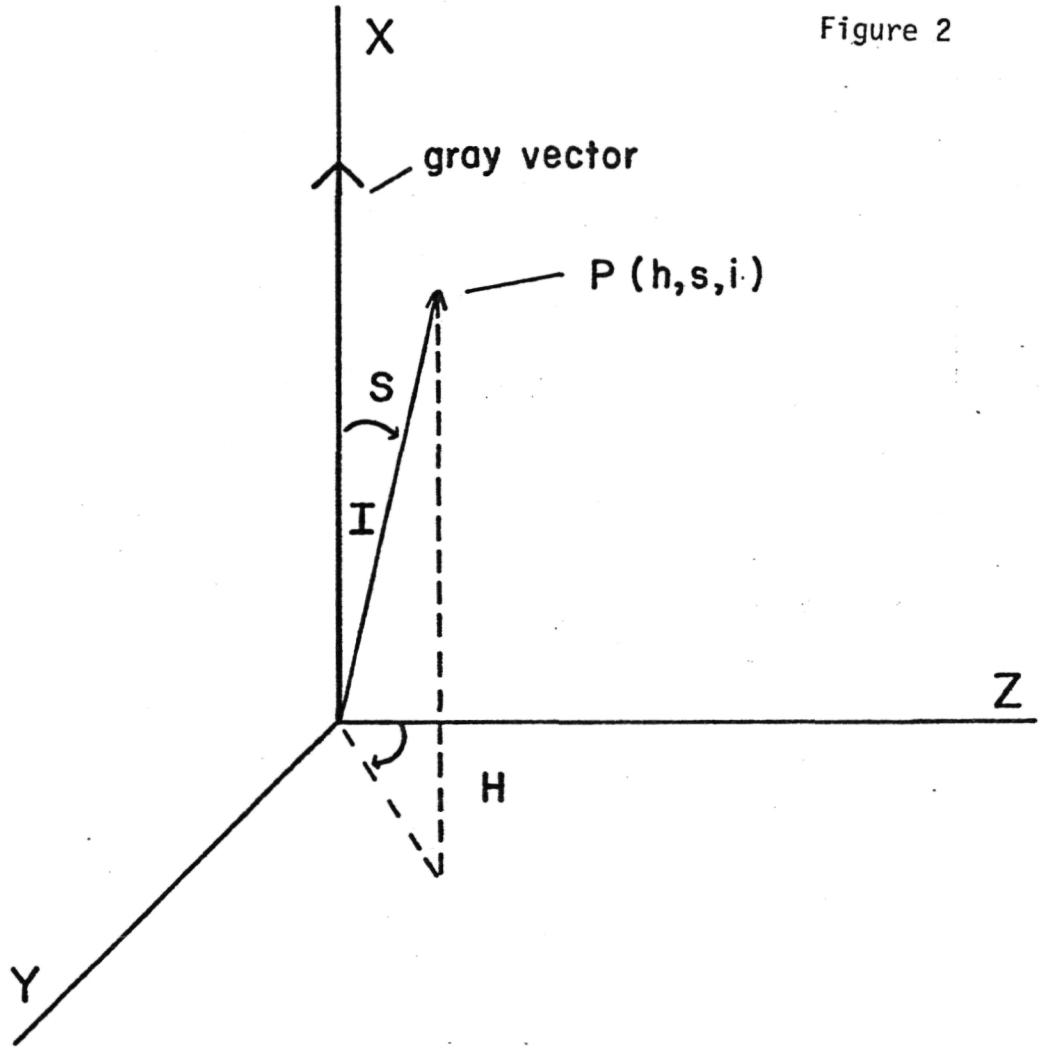

Figure 3

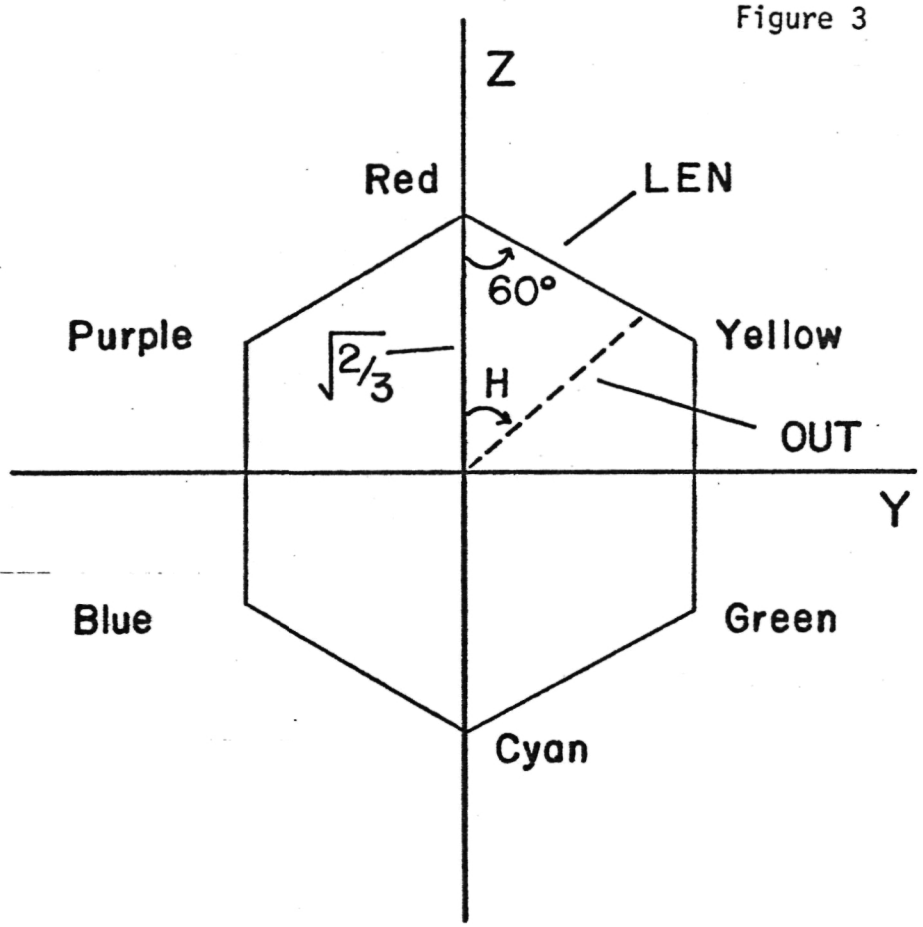

Figure 4

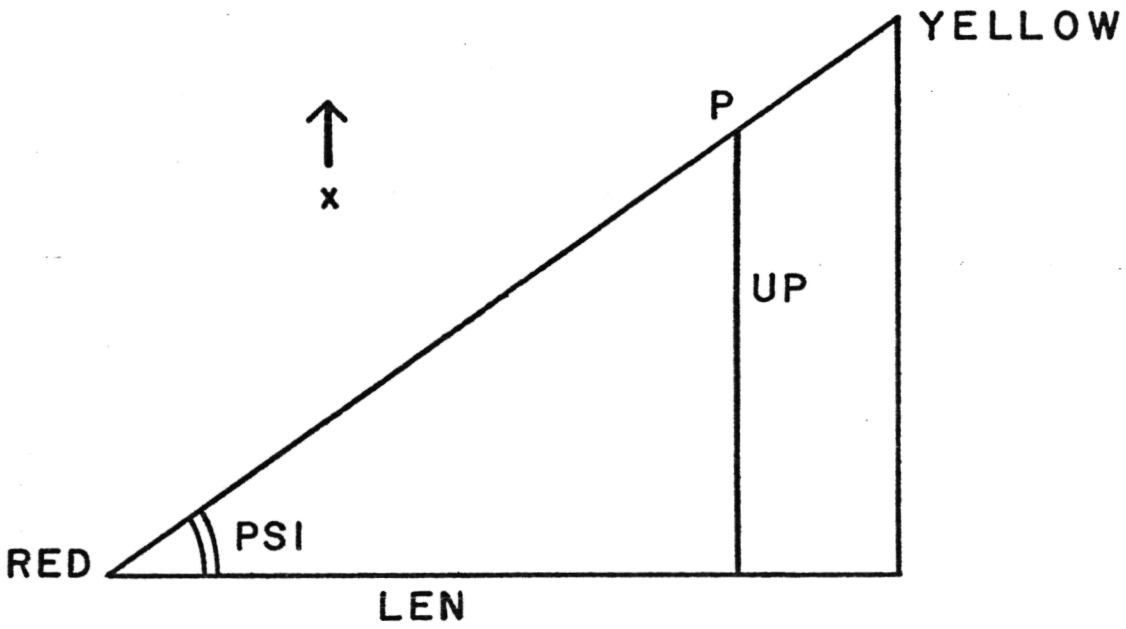

Figure 5

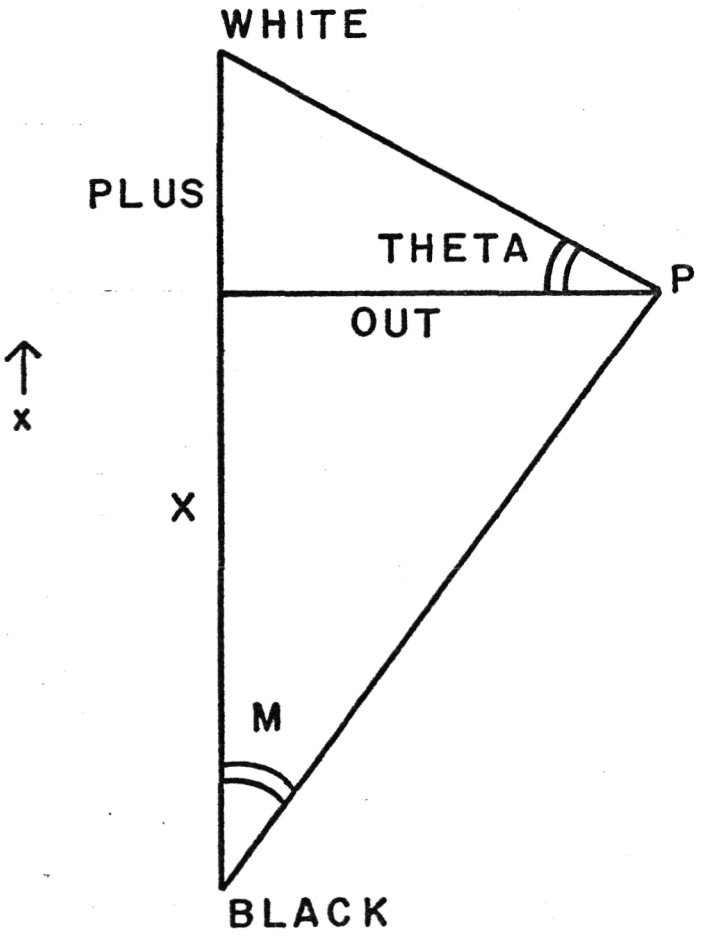

Figure 6